Long-term beach and dune evolution

Development and application of the CS-model

Hallin, Caroline

2019

Document Version:
Publisher's PDF, also known as Version of record

Link to publication

Citation for published version (APA):
Hallin, C. (2019). *Long-term beach and dune evolution: Development and application of the CS-model.* [Doctoral Thesis (compilation), Division of Water Resources Engineering]. Water Resources Engineering, Lund University.

Total number of authors:
1

Long-term beach and dune evolution

Development and application of the CS-model

CAROLINE HALLIN

FACULTY OF ENGINEERING | LUND UNIVERSITY

Long-term beach and dune evolution

Development and application of the CS-model

Caroline Hallin

LUND UNIVERSITY

Organization LUND UNIVERSITY	Document name Doctoral Thesis, report TVVR 1076
Water Resources Engineering Box 118 SE-221 00 Lund, Sweden	Date of issue April 9, 2019
Author: Caroline Hallin	Sponsoring organization Div. Water Resources Engineering

Title and subtitle
Long-term beach and dune evolution - Development and application of the CS-model

Abstract

Coastal flooding and erosion are worldwide problems that are further aggravated by rising sea levels and increasing population densities in coastal areas. In many of those areas, sandy beaches and dunes protect the hinterland from waves and extreme water levels during storms, while providing natural and recreational values. Sandy coasts are dynamic systems. Thus, risk assessments and coastal management strategies require knowledge about their long-term evolution. From coastal management and spatial planning perspectives, typically, the coastal evolution on timescales from decades up to centuries, and spatial scales in the order of kilometres are of interest. However, there is a lack of model tools integrating all the relevant processes for simulation of beach and dune evolution at these spatial and temporal scales.

In this thesis, the CS-model – a semi-empirical cross-shore sediment transport and beach and dune evolution model - is developed and tested. Included processes are dune erosion and overwash, beach-bar exchange, dune build-up through aeolian transport, and beach erosion and accretion due to gradients in longshore transport. Physics-based equations for dune erosion and overwash, beach-bar exchange, and sea level rise are have been developed and validated in previous studies. Methods to simulate the aeolian transport and morphological dune evolution are developed from established geomorphological concepts, which are translated into numerical formulations. Robust decision support should be based on probabilistic simulations for a range of future scenarios. Therefore, the CS-model is designed to be computationally efficient, through reduced-complexity transport equations and a simplified schematization of the beach profile.

The model is applied to two study sites, Ängelholm Beach in Sweden and the Kennemer Dunes in the Netherlands. In Ängelholm, the geomorphological concepts are tested against grain size and topographic data. Then, the model is calibrated and validated against a seven-year data set and the long-term beach and dune evolution from 2017–2100 is simulated for a range of sea level rise scenarios. At Kennemer Dunes, the model is applied to a 22-year data set, to study the relative importance of different transport processes for the long-term dune evolution. At Ängelholm Beach, dune erosion was found to be a dominant process for the long-term dune evolution, because the aeolian transport capacity was limited. At Kennemer Dunes, the gradients in longshore sediment transport were governing the dune volume evolution. The simulations also showed that the beach and shoreface nourishments were the most critical factors for dune growth along the long-term eroding stretches of the beach. Overall, the results are promising and suggest that the model could be a useful tool for long-term coastal risk assessment and evaluation of coastal management strategies.

Key words: Coastal processes, sediment transport, numerical modelling, Ängelholm Beach, Kennemer Dunes

Classification system and/or index terms (if any)

Supplementary bibliographical information	Language: English
ISSN and key title: 1101-9824	ISBN: 978-91-7895-062-1 (print) 978-91-7895-063-8 (pdf)

Recipient's notes	Number of pages 95	Price
	Security classification	

Signature _(signature)_   Date 2019-03-25

Long-term beach and dune evolution

Development and application of the CS-model

Caroline Hallin

LUND
UNIVERSITY

Coverphoto by Caroline Hallin

Illustrations Fig. 2.1 – 2.4 by Benjamin Fagnot

Es ist nicht genug, zu wissen, man muss auch anwenden;

es ist nicht genug, zu wollen, man muss auch tun.

Johann Wolfgang von Goethe

Table of Contents

Abstract

Coastal flooding and erosion are worldwide problems that are further aggravated by rising sea levels and increasing population densities in coastal areas. In many of those areas, sandy beaches and dunes protect the hinterland from waves and extreme water levels during storms, while providing natural and recreational values. Sandy coasts are dynamic systems. Thus, risk assessments and coastal management strategies require knowledge about their long-term evolution. From coastal management and spatial planning perspectives, typically, the coastal evolution on timescales from decades up to centuries, and spatial scales in the order of kilometres are of interest. However, there is a lack of model tools integrating all the relevant processes for simulation of beach and dune evolution at these spatial and temporal scales.

In this thesis, the CS-model – a semi-empirical cross-shore sediment transport and beach and dune evolution model - is developed and tested. Included processes are dune erosion and overwash, beach-bar exchange, dune build-up through aeolian transport, and beach erosion and accretion due to gradients in longshore transport. Physics-based equations for dune erosion and overwash, beach-bar exchange, and sea level rise are have been developed and validated in previous studies. Methods to simulate the aeolian transport and morphological dune evolution are developed from established geomorphological concepts, which are translated into numerical formulations. Robust decision support should be based on probabilistic simulations for a range of future scenarios. Therefore, the CS-model is designed to be computationally efficient, through reduced-complexity transport equations and a simplified schematization of the beach profile.

The model is applied to two study sites, Ängelholm Beach in Sweden and the Kennemer Dunes in the Netherlands. In Ängelholm, the geomorphological concepts are tested against grain size and topographic data. Then, the model is calibrated and validated against a seven-year data set and the long-term beach and dune evolution from 2017–2100 is simulated for a range of sea level rise scenarios. At Kennemer Dunes, the model is applied to a 22-year data set, to study the relative importance of different transport processes for the long-term dune evolution. At Ängelholm Beach, dune erosion was found to be a dominant process for the long-term dune evolution, because the aeolian transport capacity was limited. At Kennemer Dunes, the gradients in longshore sediment transport were governing the dune volume evolution. The simulations also showed that the beach and shoreface nourishments were the most critical factors for dune growth along the long-term eroding stretches of the beach. Overall, the results are promising and suggest that the model could be a useful tool for long-term coastal risk assessment and evaluation of coastal management strategies.

Popular science summary in Swedish

Ungefär en tredjedel av världens kuster består av sandstränder. Deras höga natur- och rekreationsvärden är välkända, men det många inte tänker på är att stränder och sanddyner även skyddar bakomliggande områden mot översvämning från havet. När havsnivån stiger till följd av klimatförändringarna ökar behovet av översvämningsskydd, men samtidigt hotas många stränder och sanddynslandskap av ökad erosion.

Erosion innebär att sand försvinner från ett kustavsnitt så att strandlinjen rör sig bakåt, inåt land. Vågor, strömmar och vindar försöker hela tiden flytta på sandkornen som hålls på plats av sin tyngdkraft. Strandlinjens läge är därför en delikat balans mellan de krafter som flyttar på sanden och de krafter som håller den kvar. Om havsnivån stiger förskjuts balansen, havet eroderar stränder och sanddyner och fyller på havsbotten med den eroderade sanden. Om havet stiger med en meter behöver en genomsnittlig sandstrand backa i storleksordningen 100 meter inåt land för att en ny jämvikt ska inställa sig.

Samtidigt som sannolikheten för översvämning och erosion ökar när havet stiger så pågår en global befolkningsförtätning i kustnära områden. Riskanalyser och planeringsunderlag kräver kunskap och prognoser om sandstränders och sanddyners utveckling och deras skyddande förmåga. För att förbättra kustskyddet förstärks ibland stränderna genom strandfodring, vilket innebär att man tillför sand till stranden från en sandtäkt ute till havs.

Inom fysisk planering och kustförvaltning är tidshorisonterna långa, från decennier upp till sekler. I de längre tidsperspektiven är även osäkerheten kring klimatförändringarna stor. Prognoserna för hur mycket havet kommer att stiga fram till år 2100 spänner över allt från ett par decimeter upp till tre meter. Vidare påverkas extrema vattenstånd och vågklimat av lufttryck och vindar, vars framtida utveckling även den är behäftad med osäkerheter.

I den här avhandlingen presenteras en datormodell som kan användas för att simulera sandstränders och sanddyners utveckling över lång tid, decennier till sekel. Modellen är snabb och robust så att många simuleringar kan köras på kort tid för att undersöka utvecklingen för flera olika klimatscenarier. Modellen simulerar hur vågor eroderar sanddynerna under stormar och ibland även spolar sand över dynerna. Den simulerar också utbytet av sand mellan strandplanet och revlar ute i vattnet och skapar så kallade sommar- och vinterstrandprofiler. På sommaren är stränderna typiskt breda, medan strandplanet på vintern är betydligt smalare eftersom vågorna har transporterat ut sanden till reveln på havsbotten. När sanden kommer tillbaka hjälper vinden till att transportera sanden upp i sanddynerna och reparera eventuella stormskador som har uppstått under vinterns stormar. Modellen

tar även hänsyn till erosion och ackumulation till följd av att sand rör sig längs med kusten, samt effekter av stigande havsnivåer.

Det finns redan idag modeller som simulerar de här processerna var för sig. Men alla dessa processer påverkar varandra och behöver därför simuleras i en integrerad modell. Det viktigaste bidraget från det här avhandlingsarbetet är att de olika processerna har kopplats ihop i en modell som kan simulera kustens utveckling över långa tidsperioder. För att kunna simulera dynernas utveckling har en ekvation utvecklats som beräknar hur mycket sand som finns tillgänglig för vinden att transportera upp i dynen. En algoritm baserad på fältobservationer styr sedan var i dynen som sanden deponeras, vilket möjliggör en dynamisk utveckling så att dynerna till exempel kan växa sig högre eller röra sig inåt land i modellen.

I avhandlingen demonstreras modellens förmåga genom tillämpning på två studieområden i Sverige och Nederländerna, Ängelholms strand i nordvästra Skåne och Kennemer-dynerna på den holländska Nordsjökusten. I Ängelholm används modellen för att simulera stranden och sanddynernas utveckling vid olika havsnivåhöjningsscenarier fram till år 2100. I Kennemer-dynerna studeras vilka processer som är viktigast för dynernas utveckling, samt hur den påverkas av mänsklig påverkan, såsom strandfodringar och byggnader på stranden.

Modellen har visat sig vara ett nyttigt verktyg som kan användas för att ta fram underlag för planering och riskanalyser i ett längre tidsperspektiv. Modellen kan också användas för att undersöka effekten av strandfodringar på stränder och sanddyners utveckling.

Acknowledgement

The ideas presented in this thesis are the outcome of generous knowledge sharing and discussions within the international coastal research community. At conferences, summer schools and visits to other universities and research institutions, the coastal research community has always been open and welcoming to me.

My two supervisors Prof. Hans Hanson and Prof. Magnus Larson have opened doors and introduced me to their contacts all over the world. Thanks for always being available for discussions and support. You are both generous, intelligent, friendly, and fun persons, whom I love to spend time with whether we discuss sediment transport equations or drink beer.

The Division of Water Resources Engineering in Lund is a great workplace with wonderful people from all over the world. Most of the time I have shared the office – and the burdens of the PhD-studies – with Dauren Mussabek. I am happy that my former co-worker from Sweco, Björn Almström also decided to pursue a PhD. You are a dear colleague and friend; I hope that we will continue working together in the future.

There are so many people in Delft that I have encountered and befriended during my PhD. Delft has a most inspiring research environment! A special thanks goes to Max Radermacher, Lotte Bontje, and Sierd de Vries at TU Delft, and Bas Huisman and Dirk-Jan Walstra at Deltares. I would also like to acknowledge my colleagues in Australia, Peter Nielsen at the University of Queensland and Patrick Hesp at Flinders University, for fruitful meetings with valuable feedback and suggestions for my work.

The Swedish coastal network is growing, and it is always a delight to spend time with colleagues from the local municipalities, consultant companies, national authorities, other universities, and the people living along the coast. The coastal section in the Swedish Association for Water and my engagement in the board have provided a valuable network and a chance to escape from the sometimes enclosed environment at the university. Thank you.

Last but not least, I would like to thank my parents, my sister and her family for putting up with a selfish workaholic, and providing a place for recreation. There is one person that I could not have managed without, my husband Björn, who only buys me flowers when my papers are rejected.

Papers

This thesis is submitted with the support of the following papers, which are referred to by their numerals in the body of text.

Appended papers

I.   Larson, M., Palalane, J., **Fredriksson*, C.**, Hanson, H. 2016. Simulating cross-shore material exchange at decadal scale. Theory and model component validation. *Coastal Engineering.* (116)57–66.

II. Palalane, J., **Fredriksson, C.**, Marinho, B., Larson, M., Hanson, H., Coelho, C. 2016. Simulating cross-shore material exchange at decadal scale. Model application. *Coastal Engineering.* (116)26–41.

III. **Hallin, C.**, Almström, B., Larson, M., Hanson, H. 2019. Longshore transport variability of beach-face grain size: implications for dune evolution. *Journal of Coastal Research.* (accepted for publication)

IV. **Hallin, C.**, Almström, B., Larson, M., Hanson, H. 2019. The relation between longshore variations in grain size distribution and sediment transport processes. *Proceedings of the Coastal Sediments Conference 2019* (accepted for publication)

V.   **Hallin, C.**, Larson, M., Hanson, H. 2019 Simulating beach and dune evolution at decadal to centennial scale under rising sea levels. *PLOS ONE* (in review)

VI. **Hallin, C.**, Huisman, B.J.A., Larson, M., Walstra, D-J.R., Hanson, H. 2019 The impact of sediment supply on decadal-scale dune evolution – Analysis and modelling of the Kennemer dunes in the Netherlands. *Geomorphology.* (accepted for publication)

*Caroline Hallin, née Fredriksson

The author's contribution to the appended papers

I.   The author contributed to the theoretical discussions, the testing and development of the model.

II.   The author conducted the case study at Ängelholm Beach and wrote the introduction, discussion, and conclusion.

III.   The author planned, conducted, and discussed the work, except for the wave model. The author wrote the manuscript.

IV.   The author planned, conducted, and discussed the work. The author wrote the manuscript.

V.   The author planned, conducted, and discussed the work. The author wrote the manuscript.

VI.   The author planned, conducted, and discussed the work, except for the wave model. The author wrote the manuscript.

Other related publications from the same author

Fredriksson, C., Martinez, G., Larson, M., Feldmann Eellend, B. 2018. Using Historical Storms for Flood Risk Management: The 1872 Storm in South Sweden. In: "Sites of Remembering: Landscapes, Lessons, Policies," edited by Lakhani, V. and de Smalen, E. *RCC Perspectives: Transformations in Environment and Society*, 3:11–17

Fredriksson, C., Feldmann Eellend, B., Larson, M., Martinez, G. 2017. The role of historical storm events in risk analysis. A study of the coastal flood events in 1872 and 1904 along the south and east coast of Scania, Sweden, *VATTEN – Journal of Water Management and Research*. 73:93-108.

Fredriksson, C., Almström, B., Hanson, H., Larson, M., Persson, O. 2017. Estimation of required beach nourishment volumes along the south coast of Sweden during 2017-2100, *VATTEN – Journal of Water Management and Research*. 73:77-84.

Lindell, J., **Fredriksson, C.**, Hanson, H. 2017. Impact of dune vegetation on wave and wind erosion. A case study at Ängelholm Beach, South Sweden, *VATTEN – Journal of Water Management and Research*. 73:39-48.

Fredriksson, C., Larson, M., Hanson, H. 2017. Long-term modelling of aeolian transport and beach-dune evolution, *Proceedings Coastal Dynamics*, 715-726

Bontje, L.E., **Fredriksson, C.**, Wang, Z., Slinger, J.H. 2016. Coastal erosion and beach nourishment in Scania as issues in Swedish coastal policy, *VATTEN – Journal of Water Management and Research*. 72:103-115.

Fredriksson, C., Tajvidi, N., Hanson, H., Larson, M. 2016. Statistical analysis of extreme sea water levels at the Falsterbo Peninsula, South Sweden, *VATTEN – Journal of Water Management and Research*. 72:129-142.

Larson, M., **Fredriksson, C.**, Hanson, H. 2016. Changing wind properties in South Sweden since the days of Tycho Brahe, *VATTEN – Journal of Water Management and Research*. 72:117-128.

Hanson, H., **Fredriksson, C.**, Larson, M. 2016. Kustordlistan.se – An Eng-Swe-Eng Coastal Dictionary for engineers and planners, *VATTEN – Journal of Water Management and Research*. 72:79–90.

Fredriksson, C., Hanson, H., Persson, O. 2014. Planning for climate change – a strategy to manage sea level rise in spatial planning in Ystad, Scania, *VATTEN – Journal of Water Management and Research*. 70:205–214.

1. Introduction

More than 10 % of the global population lives in the world's low elevation coastal zones (LECZ; <10 m elevation), and the coastal population density is rapidly increasing (Neumann *et al.*, 2015). Coastal flooding and erosion is already a major challenge along the world's coasts and is expected to further aggravate through the anticipated sea level rise (SLR) (Line *et al.*, 2014).

Sandy coasts constitute about 1/3 of the world's ice-free coastlines (Luijendijk *et al.*, 2018). They are dynamic systems where climate change and climate variations cause substantial morphological changes (Wong *et al.*, 2015). Coastal erosion is a direct threat against infrastructure and cultural, recreational and natural values; and may lead to increased risk of flooding (Bilskie *et al.* 2014). Due to the large economic values at stake and the risk to human health and lives, coastal protection has been – and will continue to be – implemented along the world's developed coastlines (Lincke and Hinkel, 2018).

Historically, mitigation measures against flooding and erosion consisted of hard structures; concrete seawalls, rubble-mound revetments, groins, dykes, *etc*. When such hard structures are introduced at sandy coasts, the sediment transport patterns are disturbed, causing loss of sandy habitats and their associated ecosystem services (Borsje *et al.*, 2011). Therefore, flexible solutions, where sand and vegetation are used to strengthen beaches and dunes, are today the preferred method for coastal protection in many countries (Hanson *et al.*, 2002). Coastal management strategies are changing towards working with natural processes instead of against them (de Vriend *et al.*, 2015).

Risk assessments and design of coastal protection depend upon predictions of long-term beach and dune evolution. Therefore, it is essential to understand the dynamics of sandy coasts when exposed to climate change and climate variations. From the perspective of coastal management and spatial planning, timescales from decades up to centuries are of interest (Stive *et al.*, 2002). The level of detail in the predictive tools should be appropriately selected considering the uncertainty of the forecasted forcing.

Because the future is uncertain, probabilistic rather than deterministic approaches are preferred (Wainwright *et al.*, 2015). To be able to generate multiple predictions that cover a range of possible future scenarios for the beach and dune system, robust,

computationally efficient model tools are required, which couple nearshore, beach, and dune processes.

1.1. Coastal evolution models

Numerical models of coastal morphological processes can be divided into empirical, semi-empirical, and process-based models. There is not a clear division between the different types of models; it is a sliding scale from statistical black-box type approaches towards detailed physical descriptions of all relevant hydro- and morphodynamic processes.

Coastal evolution can be described in a range of dimensions, from 1D-models of coastlines or cross-shore transects to full 3D representations (Hanson *et al.*, 2003; Lesser *et al.*, 2004). The choice of model depends on the process of interest and the studied time and spatial scale, where the level of detail in the model should be appropriate for the study. The model extent can be limited to the nearshore, the beach, or the dune, or a combination of them. Typically, different transport processes, such as dune erosion, longshore transport, and aeolian transport are simulated with separate model tools.

Beach and dune erosion during storms are typically simulated on timescales of hours to days with process-based (*e.g.* XBeach; Roelvink *et al.* 2009), or semi-empirical (*e.g.* SBeach; Larson *and* Kraus 1989) cross-shore beach profile models. Long-term coastal evolution due to gradients in longshore transport is modelled with coastline models based on one-line theory (Pelnard-Considère, 1956) such as GENESIS (Hanson and Kraus, 1989), Unibest CL+ (Tonnon *et al.*, 2018), or Litpack (DHI, n.d.). Numerical modelling of aeolian transport and morphological dune processes is not as well-developed, but have seen advances in the latest two decades (Hoonhout and de Vries, 2016; Luna *et al.*, 2011; van Dijk, Arens, and van Boxel, 1999). However, simulation of the decadal beach and dune evolution requires models where transport processes in the dunes, beach, and nearshore are dealt with integrally to account for the different response timescales and feedback mechanisms of beaches and dunes (Sherman and Bauer, 1993).

Recently, two new model concepts have been developed that couple cross-shore and longshore transport processes at decadal timescales, the CoSMoS-COAST model (Vitousek *et al.*, 2017) and the LX-model (Robinet *et al.*, 2018). They are based on a coupling of the one-line concept (Pelnard-Considère, 1956) and a cross-shore equilibrium model driven by changes in the wave climate (Yates *et al.*, 2011). Both models show promising results, however, they do not include dune processes.
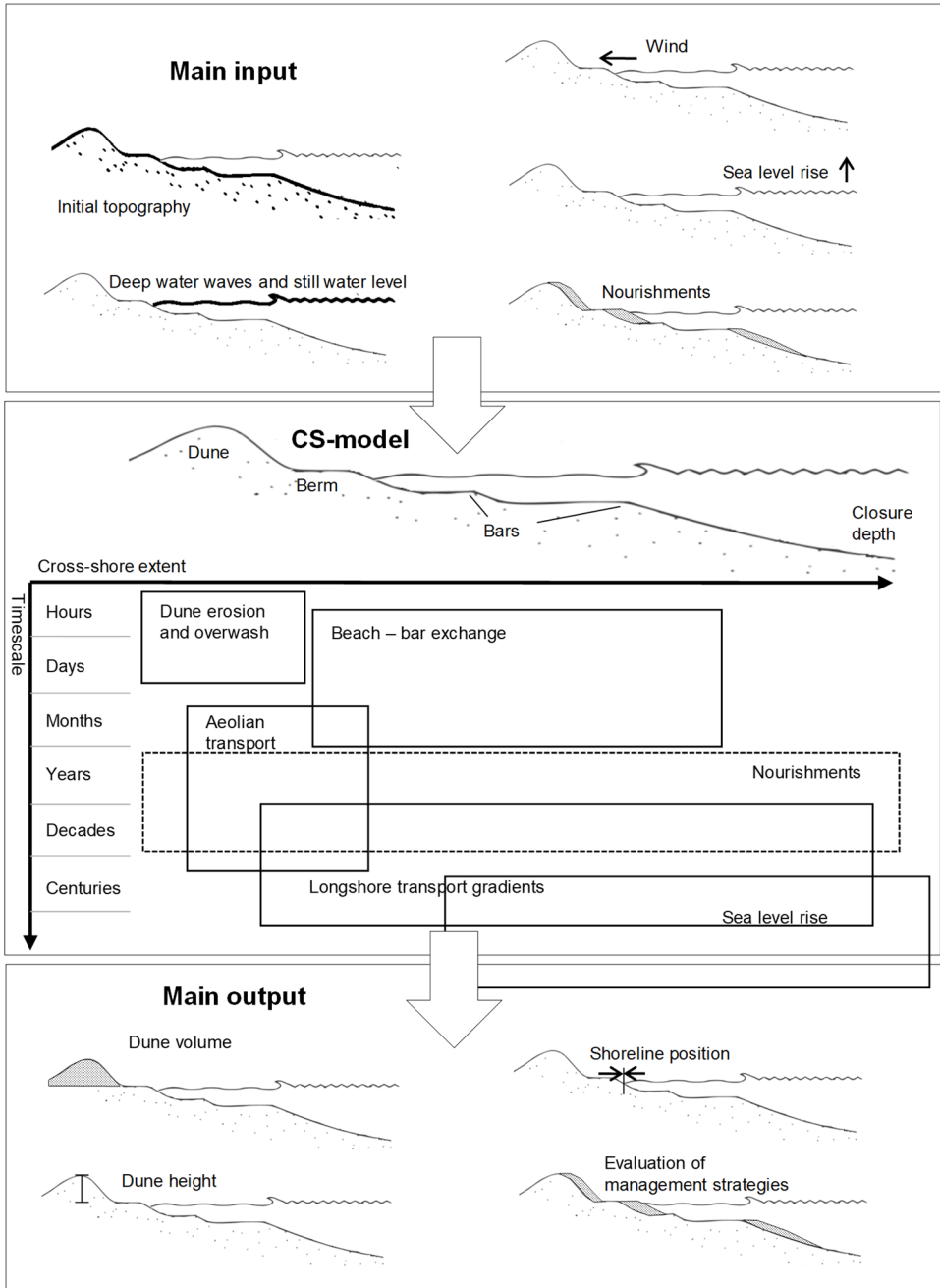
Zhang *et al.* (2015) combined a cellular automata model, simulating aeolian transport and dune growth, with process-based, profile-resolving longshore and cross-shore transport models in the subaqueous. The model successfully simulated long-term dune evolution at a study site on the Polish coast, however, the model has a high degree of complexity, which is not always desired in engineering applications. A more simplistic dune evolution model is the PCR model by Ranasinghe, Callaghan, and Stive (2012). The PCR model combine the processes of dune erosion and dune recovery with SLR through a probabilistic approach (Callaghan *et al.*, 2008), where the probability of dune erosion increases with SLR. However, the dune recovery rate is considered as a result of constant aeolian transport and longshore transport processes are not considered.

Among the most commonly used models for long-term predictions of beach and dune evolution, there is still missing a model that bridges the gap between nearshore, beach, and dune processes on timescales relevant from a coastal management perspective. For this purpose the CS-model, as presented in this thesis, was developed.

1.2. The CS-model

The CS-model is a numerical model with the capability to simulate beach and dune evolution at decadal to centennial timescales. The CS-model includes the relevant sediment transport processes that impact the beach and dune evolution; dune erosion and overwash, aeolian dune build-up, beach-bar exchange, beach erosion and accretion due to gradients in longshore sediment transport, and response to sea level rise. This thesis describes the development and application of the CS-model, with emphasis on aeolian transport, morphological dune evolution, and the impact of sea level rise.

Figure 1.1 displays a schematic illustration of the CS-model. The included processes are active in different parts of the cross-shore profile and over a range of timescales. The coastal evolution is simulated in single or multiple cross-shore transects, which enables the model to represent coasts in length scales of kilometres. Model output consists of parameters relevant for coastal management such as shoreline change, dune volume, and dune height. Future beach and dune evolution can be investigated through varying input parameters, such as wind speed, wind direction, waves, and water levels. The effect of different nourishment strategies may be investigated through varying the placement, frequency, and volume of nourishment.

Main input

Wind

Initial topography

Sea level rise ↑

Deep water waves and still water level

Nourishments

CS-model

Dune

Berm

Bars

Closure depth

Cross-shore extent

Timescale

Hours	Dune erosion and overwash	Beach – bar exchange
Days		
Months	Aeolian transport	
Years		Nourishments
Decades		
Centuries	Longshore transport gradients	Sea level rise

Main output

Dune volume

Shoreline position

Dune height

Evaluation of management strategies

Figure 1.1
The CS-model concept; required input, included processes and their timescales, and the main output from a coastal management perspective.

The CS-model builds on a set of physics-based semi-empirical equations, which require data for calibration and validation. The more data that is available from the coast of interest, the more accurate predictions can be made. This holds for all models, but especially semi-empirical models – like the CS-model – require site-specific data to deliver somewhat reliable results.

1.3. Objective

The objective of this thesis work is to develop a numerical model with the capability to simulate beach and dune evolution at time-scales of decades to centuries and spatial scales of kilometres.

The development of the CS-model is a collaborative work within the coastal engineering group at Lund University. The focus of this thesis work and the main contribution from the author is the development of the simulation of aeolian transport, morphological dune evolution, and the impact of sea level rise to reach the overall objective.

1.4. Thesis structure

This thesis is a compilation thesis, consisting of an introductory summary of the thesis work and five appended papers.

Paper I and II form a basis for this thesis. Paper I introduces the CS-model concept, and in paper II, the model is tested on three different case studies in Sweden, Portugal, and Mozambique. The original version of the CS-model is based on previously developed and validated concepts, which are combined to generate new capabilities.

In paper III and IV, theories about grain-size sorting and how it relates to beach and dune processes are described and tested in a case study at Ängelholm Beach, Sweden.

In paper V, the CS-model is extended to account for sea level rise, and the profile schematization, the aeolian transport, and the morphological evolution of the dune are improved. The new scheme for aeolian transport builds on the theories about grain-size sorting that were presented in paper III. The model is applied to investigate the impact of sea level rise on beach and dune evolution from today until 2100 for three different IPCC scenarios at Ängelholm Beach.

In paper VI the CS-model is applied to a study site in the Netherlands to investigate the impact of sediment supply on dune evolution.

The thesis starts in chapter 2 by describing the theoretical background for the CS-model components (paper I, III, IV, and V). In chapter 3, the CS-model is described in detail (paper I, V and VI). The case study sites, Ängelholm Beach in Sweden and the Kennemer dunes in the Netherlands, are introduced in chapter 4 (paper II, III, IV, V and VI). The results of the grain-size analyses and model applications are briefly discussed in chapter 5 (paper III, IV, V, and VI), followed by conclusions and suggestions for future work in chapter 6.

The symbols and abbreviations used throughout the thesis are collected in a list of symbols at the end. The individual papers have separate symbols lists.

2. Theoretical background

This chapter gives a theoretical background for the physical processes included in the CS-model and presents the results of the literature study, which provides the basis for the development of aeolian transport and morphological dune evolution.

2.1. Dune erosion and overwash

The impact of waves on dunes can be divided into four different types according to the storm impact scale (Sallenger, 2000); swash, collision, overwash, and inundation (Figure 2.1).
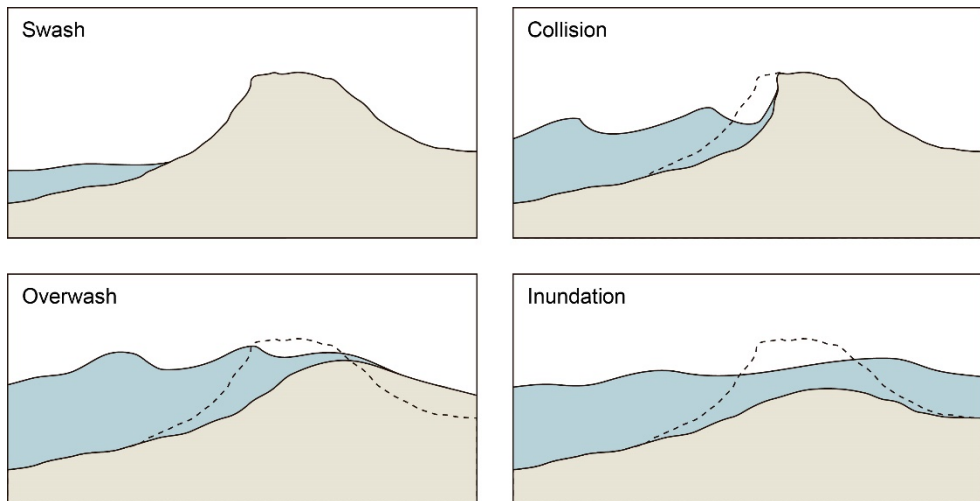
Figure 2.1
The storm impact scale for barrier islands by Sallenger (2000).

In the swash regime, the waves only reach and erode the foreshore and do not impact the dune. In the collision regime, wave run-up collides with the base of the dune; sediment is eroded from the dune and deposited on the beach or transported offshore. During overwash, the waves reach over the foredunes and wash sand

landwards at the same time as sediment is eroded from the dune as for the collision regime. Inundation means that the entire front dune ridge is inundated with water; the dune is then impacted by surf-zone like processes (Sallenger, 2000).

Dune erosion is a threat to the coastal safety, and subsequently, many analytical and numerical methods have been developed to quantify dune erosion due to the impact of waves and water levels (Larson, Erikson, and Hanson, 2004). The analytical models are based on the equilibrium profile (Kriebel and Dean, 1993; Steetzel, 1993; Vellinga, 1986) or wave impact approach (Larson, Erikson, and Hanson, 2004; Nishi and Kraus, 1996; Overton, Fisher, and Young, 1988). The equilibrium approach assumes that the beach adjusts towards an equilibrium state with the wave and water level conditions (Bruun, 1954; Dean, 1977). The new equilibrium is approached through erosion of sediment from the beach and the dune, and deposition in the subaqueous part of the profile (Vellinga, 1986). In real situations, storm surges and wave conditions are time-varying, and the storm durations typically are too short to reach a storm equilibrium profile (Larson, Erikson, and Hanson, 2004).

The wave impact approach is a more physics-based method, assuming that the dune erosion is a function of the frequency and intensity of wave impact. The eroded weight (or volume) of sediment is assumed to be proportional to the force acting on the dune, where the force equals the change of momentum flux of the bores impacting the dune (Overton, Fisher, and Young, 1988). Based on this concept, Larson, Erikson, and Hanson (2004) derived an analytical model where the dune erosion is proportional to the square of the runup height exceedance above the dune toe. The impact equation is combined with a Hunt-type runup equation so that the dune erosion can be computed from deep-water wave conditions in combination with still water levels (SWL), which is practical for engineering applications. Following a site-specific calibration of the empirical coefficient in the formula, the model showed good agreement with both field data and laboratory data (Larson, Erikson, and Hanson, 2004).

The advantage of analytical models is that they are easy to use and fast to apply with a small amount of required input data, making them suitable for approximate estimations over large spatial scales. In more detailed studies, numerical methods such as SBeach (Larson and Kraus, 1989) or XBeach (Roelvink *et al.*, 2009) are commonly used. SBeach simulates profile evolution during storms based on a profile equilibrium concept, primarily focusing on changes to the berm and bar. The morphological evolution is related to wave, water level, and sediment properties, through empirical equations. Dune erosion is induced through avalanching of the dune front, which is triggered by an exceedance of a critical slope due to offshore transport from the berm by swash processes.

In the case of significant alongshore variability, 2D approaches may be required (Roelvink *et al.*, 2009). In Xbeach, 2DH (*i.e.* two horizontal dimensions) equations are solved for wave propagation, flow, and sediment transport for time-varying wave and current boundary conditions. Dune erosion is initiated through avalanching, when a critical bed slope for wet (milder) or dry (steeper) conditions is exceeded; the avalanching process is typically triggered by high infragravity waves, partly inundating the dune slope (Roelvink *et al.*, 2009).

The numerical models typically require more computational effort and user skill than the analytical models. Following the objectives, and relevant time and spatial scales of the CS-model, a reduced complexity analytical model is preferred. The analytical dune erosion model by Larson*, Erikson, and Hanson (2004) is therefore implemented in the CS-model, within each time step during which the conditions are constant. It offers a physics-based, yet simple schematization of a complicated process. However, the performance of the model is dependent on access to data for calibration of the empirical coefficient, which differed by an order of magnitude between the different test cases (Larson, Erikson, and Hanson, 2004).

Analytical models of overwash have not been as widely developed and used (Larson *et al.*, 2009). Analogous to the dune erosion processes, numerical models, such as Xbeach, can be used to calculate overwash, but is not compatible with the CS-model concept. Instead, Larson's analytical dune erosion model has been extended to account for overwash (Larson *et al.*, 2009). The overwash method is based on the same physical description of wave impact as the erosion model. Since a portion of the uprushing water is passing over the dunes, the wave impact on the dune front is assumed to decrease. A correction factor, given by the ratio between the dune crest height and the runup height above the dune foot, is applied to decrease the erosion rate. The overwash portion of the eroded sediment is assumed to be deposited on the landward dune slope.

The equations for dune erosion and overwash (Larson *et al.*, 2009; Larson, Erikson, and Hanson, 2004) are presented in the model description chapter, in section 3.2.

2.2. Beach-bar exchange

In the previous section, analytical and numerical models to estimate dune erosion and offshore transports during storms were discussed. When considering beach evolution at time-scales longer than singular storm events, both onshore and offshore transport are relevant to consider.

Seasonal changes in wave climate typically generate so-called summer and winter beach profiles (Figure 2.2), also known as berm and bar profiles, respectively

(Shepard, 1950). During the fall and winter months – when storm surges and large wave heights occur more frequently – sediment is transported offshore from the upper part of the profile, leading to berm and dune erosion and the creation of an offshore bar. During seasons with calmer wave climate, the sand slowly returns from the bar to the berm, so that the beach and dune recover.
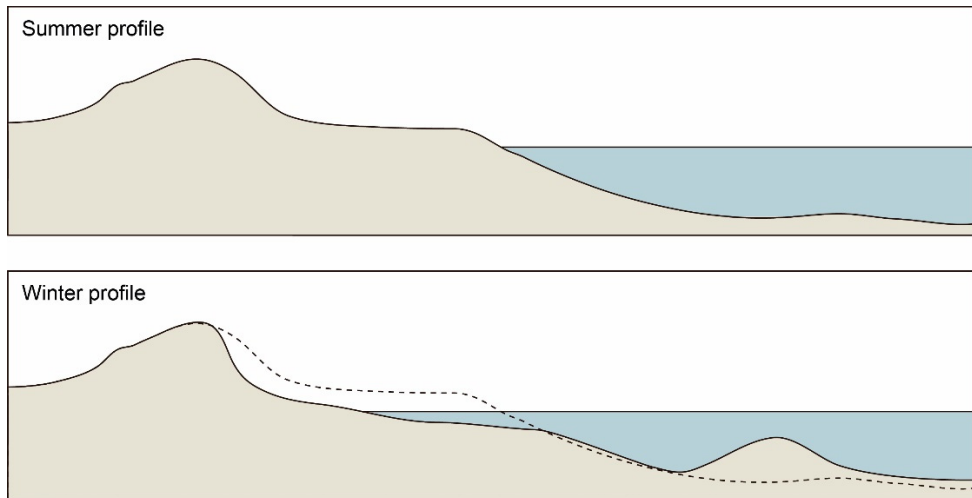
Figure 2.2
Characteristic summer and winter profiles.

Whether sediment will move onshore or offshore depends on the balance between the constructive (onshore) and destructive (offshore) forces. The process can in a simplified manner be described as a balance between the onshore movement of sediment due to the asymmetry of the wave oscillatory velocities, and the offshore movement due to gravity and return flow (see, *e.g.* Bailard 1982). The cross-shore transport direction has in many studies been found to depend on some variation of the Dean parameter, $H/(wT)$, where H is the deep water wave height, w is the sediment fall speed, and T is the spectral peak period (Seymour and Castel, 1989); offshore transport for higher values and onshore transport for lower values.

Considering the complexity of surf zone processes, a full description of the cross-shore transport processes in long-term numerical models is not practical due to computational efficiency. Instead, equilibrium-based models are typically employed, where the beach and bar exchange is related to the wave climate and sediment characteristics.

In the most simple case, shoreline change can be described as a function of the deviation of the actual shoreline from the shoreline in equilibrium with the wave climate (*e.g.* Miller and Dean 2004; Yates *et al.* 2011). A similar physics-based

approach was developed by Larson and Kraus (1989), in which the cross-shore transport is related to an equilibrium bar volume instead of an equilibrium shoreline position. Offshore transport decreases as the bar grows, in agreement with the increased wave energy dissipation over the bar. The equations for beach-bar exchange following the method by Larson and Kraus (1989) and Larson, Hanson, and Palalane (2013) are presented in the model description chapter, in section 3.3.

2.3. Longshore sediment transport

The previous sections discussed sediment transport in the cross-shore direction. Cross-shore transport gives rise to morphological changes on the seasonal, tidal cycle, or event scale. However, the beach profile typically recovers after erosion events, unless the sediment budget is not in balance. Longshore sediment transport processes in combination with sediment supply or deficit – due to shoreline orientation, transport in rivers and lagoons or interruption by structures – is a common cause of an imbalance of the beach sediment budget. A positive gradient in the longshore transport along a sandy beach causes erosion, and a negative gradient causes accretion.

The wave-generated longshore current is formed by waves breaking with an oblique angle towards the shore (Figure 2.3). The generation of near-shore currents can be explained by gradients in the radiation stresses, defined as the mean excess momentum-flux due to the presence of waves (Longuet-Higgins and Stewart, 1964). The radiation stress gradients are significant drivers for nearshore transport processes, both in the cross-shore and longshore direction. However, the tide and the wind may also drive longshore currents. The wave breaking stirs up the sediment and the longshore current transports the sediment alongshore. Swash transport from oblique waves, so-called beach drift, also contributes to the longshore transport.
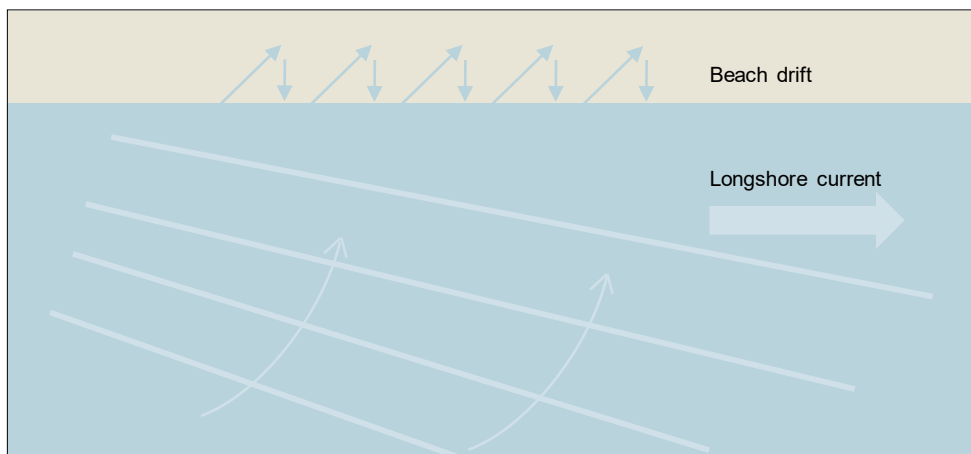
Figure 2.3
Schematic picture of longshore sediment transport due to longshore current and swash processes.

Longshore transport rates can be computed through semi-empirical equations (Inman and Bagnold, 1963; Kamphuis, 1991); in the most simple case just relating the transport to the breaking wave height and angle (USACE, 1984). Several numerical models exist that combine the transport equations with a sediment balance equation to compute coastline evolution, *e.g.* GENESIS (Hanson and Kraus, 1989), Litpack (DHI, n.d.) and Unibest CL+ (Tonnon *et al.*, 2018). These models are based on the one-line concept (Pelnard-Considère, 1956), which assumes that the active beach profile has a constant shape. This assumption implies that the shoreline, and all other contour lines across the profile, move in parallel; landward in case of erosion and seaward in case of accretion. The active beach profile is typically defined vertically from the berm crest to the depth of closure (Hanson and Kraus, 1989).

The longshore transport impacts not only the beach sediment budget but also the grain-size composition. Transport processes sort sediment through selection by weight and grain size during pick up and deposition (Trask and Hand, 1985). Finer particles are more easily entrained, leading to coarsening of sediment in eroding areas and accumulation of finer sediments where the sand is deposited (Self, 1977).

In the CS-model, routines to compute longshore transport has not yet been included. Transports rates are added as constant sources or sinks based on observations of long-term volume or shoreline change rates. Sediment sorting due to longshore transport gradients is accounted for in the routines for aeolian transport.

2.4. Sea level rise

Due to SLR, larger waves approach the shore leading to increased sediment transport offshore. The concept of an equilibrium profile that adjusts to SLR, causing shoreline retreat, is known as the Bruun Rule (Bruun, 1962, 1954). The Bruun Rule is based on the assumption that SLR creates accommodation space for sediment within the subaqueous part of the active profile.

The Bruun Rule provides a simple method to estimate the shoreline retreat, R_{Bruun}, under a slowly rising sea level (Bruun, 1962), $R_{Bruun} = S_{SLR}(B_{Bruun}/h)$, where S_{SLR} is the sea level rise, B_{Bruun} and h the width and the height of the active profile, respectively (Figure 2.4). The width B_{Bruun} represents the distance from the shoreline to the depth of closure, and h is the sum of the closure depth and berm height (Bruun, 1962).
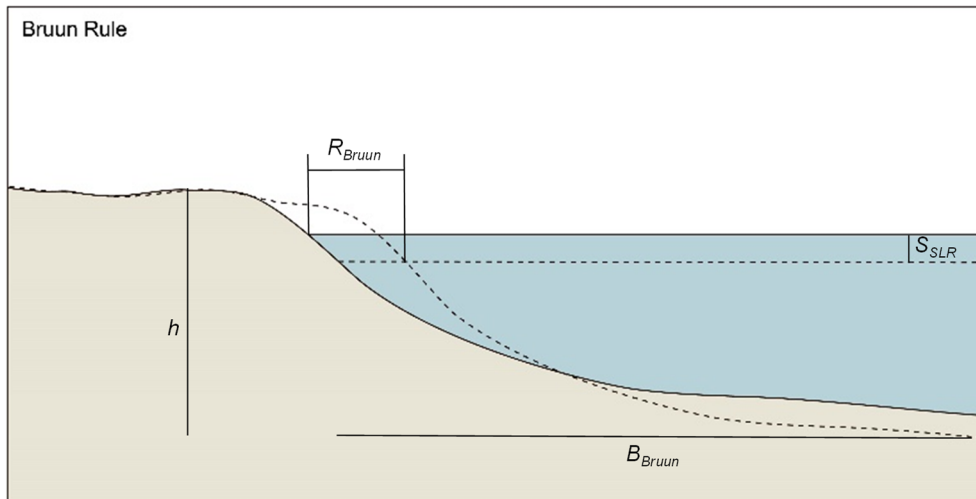
Figure 2.4
Schematization of the Bruun rule. A sea level rise, S_{SLR} cause a shoreline retreat equal to R_{Bruun}.

The Bruun Rule assumes that the profile consists entirely of sand with no longshore transport gradient, that there is a full spectrum of waves, wind and water levels to force the profile to its new equilibrium, and that the SLR is slow. All sediment transport is in the seaward direction and dunes are not considered.

Some of these simplifications imply problems when applying the Bruun Rule in engineering projects. For example, infilling sediment can come from various sources, not only the beach. The sediment may also originate from a positive longshore sediment transport gradient, artificial nourishment, or from offshore

supplies outside the depth of closure, also known as the Dean equilibrium concept (Dean, 1987). The latter has for example been observed in Florida where sediment from offshore sand waves has been transported onshore during extreme storm events (Dean and Houston, 2016; Houston, 2015). However, these processes are more common at geological timescales than at engineering timescales, if known to be present they could, in a numerical model, be added as a sediment source for the beach or bar volume.

Further, the Bruun Rule does not take into account any beach-dune interaction. Davidson-Arnott (2005) proposed the RD-A Model, which is a development of the Bruun Rule, building on the same underlying assumptions, but it also includes a foredune behind the beach. The RD-A model describes a transgression that is similar to that of the Bruun Rule. The RD-A Model assumes that all sediment eroded from the dune will be transported to the landward side, allowing the dune to retreat. The dune foot and the dune crest are assumed to increase with the same height and pace as the SLR and thus maintaining the dune volume.

Rosati, Dean, and Walton (2013) developed the Bruun Rule further by adding landward transport due to wind and overwash, keeping the assumption of seaward transport driven by a deviation from the equilibrium profile shape.

The Bruun Rule is widely used for engineering applications but is also a much-discussed concept within the scientific community (Cooper and Pilkey, 2004). The main argument against the Bruun Rule concerns its two-dimensionality and the assumption that other transport processes such as gradients in longshore transport and overwash are excluded. However, this critique is not relevant if the Bruun Rule is applied only to compute the accommodation space for sediment within the active profile. Other relevant transport processes can be dealt with in separate transport equations since the morphological evolution of the beach and dune is a result of all of these types of transports.

Another common critique against the Bruun Rule is the question of the validity of the concepts of equilibrium profiles and depth of closure. The concept of an equilibrium profile has been supported by many field investigations (Bruun, 1954; Dean, 1977) and is a widely used method for profile schematization in long-term model applications. In a recent extensive laboratory study, both the original Bruun Rule (Bruun, 1962) and the modified version including landward transport (Rosati, Dean, and Walton, 2013) showed good agreement with observations (Atkinson *et al.*, 2018) and confirmed the underlying assumption of a profile adjustment to SLR.

The CS-model assumes an equilibrium profile in the subaqueous, and therefore the Bruun Rule concept fits well in the model. In numerical modelling, the accuracy gained from more realistic profile representations needs to be balanced against a higher degree of model complexity, which typically is more computationally

expensive. It is, however, essential to keep the limitations of the equilibrium concept in mind when applying the CS-model and the Bruun Rule.

2.5. Dune build-up

The mechanics of sediment transport by wind and the associated morphological evolution of coastal dune systems have been studied extensively (*e.g.* Bagnold 1941; Hesp 1988), which has provided profound insights to aeolian transport processes (Durán, Claudin, and Andreotti, 2011). Still, existing models are unable to predict transport rates at timescales of months to years (Barchyn *et al.*, 2014; de Vries *et al.*, 2012; Sherman and Bauer, 1993). The commonly used formulas for wind transport tend to overestimate the transport rate when compared to field observations (Barchyn *et al.*, 2014; Sherman *et al.*, 1998). Furthermore, transport rates alone cannot be used to predict the morphological evolution of foredunes. In long-term beach-dune evolution, it is also important where the aeolian sediment is deposited in the foredune, on the crest, seaward – or landward slope, or if it is transported beyond the active profile and lost from the system.

Sherman and Bauer (1993) stated that foredune morphology primarily depends on the wind climate, magnitude and frequency of wave attack, characteristics of beach sediment, and vegetation. Other factors found to influence aeolian transport, and thus foredune morphology, is sediment availability (Psuty, 1988), beach width and fetch length (Bauer *et al.*, 2009), surface moisture (Bauer *et al.*, 2009), snow and ice cover (Ollerhead *et al.*, 2013), crust development on beach surface (Hoonhout and de Vries, 2016), and grain size (Bagnold, 1937).

Several conceptual models have been put forward to describe long-term dune evolution under the influence of aeolian transport (*e.g.* Davidson-Arnott 2005; Psuty 1988; Sherman and Bauer 1993) of which a few are translated into numerically solved predictive models (*e.g.* Durán and Moore, 2013; Sauermann*,* Kroy, and Herrmann, 2001; van Dijk*,* Arens, and van Boxel, 1999). Process-based numerical dune evolution models (Luna *et al.*, 2011; Sauermann, Kroy, and Herrmann, 2001; van Dijk, Arens, and van Boxel, 1999) combine airflow simulations based on the Navier-Stokes equations (van Boxel, Arens, and van Dijk, 1999; Weng *et al.*, 1991) with equilibrium transport formulas (Bagnold, 1937; Lettau and Lettau, 1978). Further, Hoonhout and de Vries (2016) recognised that aeolian processes forming the dunes depend strongly on the supply of sediment from the beach. They introduced Aeolis, a model that simulates bed surface processes and sediment availability in grid cells across the beach.

The process-based dune models, provide detailed physical descriptions of aeolian sediment transport and dune evolution; also under the impact of vegetation (Luna *et al.*, 2011; van Dijk, Arens, and van Boxel, 1999). However, their level of detail and schematization of the topography is not compatible with the CS-model concept. Decadal simulations require computationally efficient models with a two-way exchange of sediment between the beach and the dune (Psuty, 1988). In the following, the literature on the mechanics of wind-blown sand and limiting factors is examined with the purpose to derive a new, reduced-complexity method to simulate dune build-up that is compatible with the CS-model structure and the included transport processes.

2.5.1. Equilibrium transport formulas

Aeolian transport occurs when the forces acting to lift a grain of sand exceeds the force of gravity (Figure 2.5). When the conditions for initiation of motion are met, the sediments can be transported in at least four different modes (Bagnold, 1941). (1) creep: the grains are rolling on the surface; (2) saltation: sand grains are lifted and makes a jump through the air; (3) reptation: sand grains that are too heavy to be lifted by the wind are set in motion by saltating grains; and (4) suspension: very fine sand may be transported short distances in suspension.
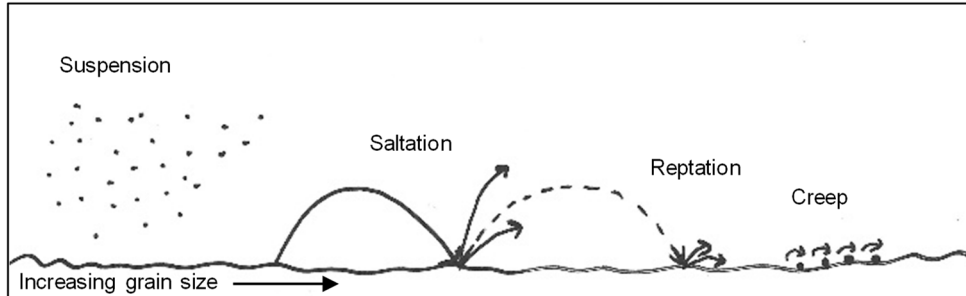
Figure 2.5
Schematic pictures of initiation of motion and different modes of aeolian transport.

There are several equations describing aeolian sediment transport rates at equilibrium conditions, *i.e.*, fully developed saltation, of which most relates the aeolian transport rate to grain size, wind shear velocity, and a critical wind shear velocity for initiation of motion (*e.g.* Bagnold 1937; Hsu 1971; Kawamura 1951; Lettau and Lettau 1978; Owen 1964; Zingg 1953). Sherman *et al.* (2013) calibrated these equations against field data and found that calculated transport differed by an

order of magnitude depending on the choice of formula. The formula by Lettau and Lettau (1978) had the best fit compared to the investigated data set.

Sediment transport formulas that are only accounting for wind speed and grain size are commonly overestimating transport rates when compared to field data from beach environments (de Vries *et al.*, 2012; Sherman *et al.*, 1998). Wind speed, wind direction, and moisture content are constantly varying at sandy beaches (Bauer *et al.*, 2009), and both their spatial and temporal variabilities are considered to be important in aeolian sediment transport models (Barchyn *et al.*, 2014). Moreover, de Vries *et al.* (2012) concluded that in modelling yearly to decadal sediment transport rates, limiting parameters are of interest, rather than time-varying forcing conditions. As it has been proved difficult to model aeolian transport, limiting factors are thus crucial in order to construct stable long-term models. Such limiting factors, which are not included in the equilibrium aeolian transport models mentioned above, are beach slope, beach width, vegetation, and sediment availability. They are discussed in more detail in the following sections.

2.5.2. Beach slope

The beach slope affects aeolian sediment transport because more wind shear stress is needed to move sediment uphill. Several formulas, which are derived from laboratory data, describe the impact of slope on aeolian transport (Bagnold, 1973; Hardisty and Whitehouse, 1988; Iversen and Rasmussen, 1994). De Vries *et al.* (2012) studied how dune growth varied with average beach slope in nature, from mean water level to the dune foot, and found a positive correlation between milder beach slopes and yearly transport rates. However, the effect of beach slope is difficult to distinguish in field data due to the co-variation with fetch length, grain size, and beach sediment availability, which also influence aeolian transport.

Short and Hesp (1982) coupled the beach-dune sediment exchange to the concept of morphodynamic beach states by Wright and Short (1984), assuming that the aeolian transport was influenced by beach slope, grain size distribution, and beach width. Dissipative beaches have relatively wider, milder sloping beaches and finer grain size resulting in larger aeolian transport rates. Thus, dissipative beaches have vast dune landscapes and reflective beaches minimal dune development (Short and Hesp, 1982). Sherman and Bauer (1993) calculated the potential aeolian transport to be 140 % higher at a dissipative beach than on a reflecting beach, accounting for differences between characteristic values of grain size and beach slope between the different beach types.

On the contrary, Sherman *et al.* (1998) found that neglecting the impact of grain size, the effect of slope correction on transport rates at beaches with slopes below 15° is small. Since most berm and foredune slopes are well below that limit, slope

impact is here assumed negligible when modelling transport rates to the foredune on long timescales.

2.5.3. Fetch

When studying the wind field alone, sediment transport would be largest on the foreshore, where the wind shear stress is higher, and decrease in the downwind direction due to boundary layer development (Bauer *et al.*, 2009). Though, to reach the transport rates described by the equilibrium equations, a critical fetch length is required. This is due to the mechanism of the saltation process, which needs to adjust over a critical distance for the equilibrium conditions to become fully developed. Field measurements confirm that the actual transport is increasing with distance from the water line, which can be explained by decreasing surface moisture and initiation of saltation processes (Bauer *et al.*, 2009). In the same study, a decrease in transport was observed on the upper part of the beach, close to the foredunes, probably due to the boundary layer development.

The actual fetch length on the beach depends on the dry beach width, which can be defined as the distance from the runup limit to the dune foot, adjusted for the angle of attack of the wind. The aeolian transport is assumed to increase with increasing fetch up to a critical fetch length where the equilibrium transport rate is achieved. In a field experiment at Greenwich Dunes, Prince Edward Island National Park in Canada, the critical fetch length was determined to be in the range of 50–150 m (Bauer *et al.*, 2009). The critical fetch length is found to increase with wind speed. At Long Point, Lake Erie, Canada, the critical fetch was determined to 15 m and 30 m for wind speeds of 5.8 m/s and 8.5 m/s respectively and for a wind speed at 13.9 m/s the critical fetch was not reached over a 40 m wide beach (Davidson-Arnott and Law, 1990).

Equilibrium conditions are rarely reached, as many beaches are narrower than the critical fetch length and internal boundary layers develop over the beach, reducing shear velocity in the downwind direction (Bauer *et al.*, 2009). Wind from oblique angles, therefore, become an important factor for aeolian transport as the fetch distance increases with the wind angle for oblique angles of 0–90° from a shore-normal (Bauer and Davidson-Arnott, 2002; Delgado-Fernandez and Davidson-Arnott, 2011). However, the increase in transport due to the prolongation of the fetch is counteracted by a reduction due to the cosine effect, as the actual transport to the dune depends on the onshore transport component (Bauer and Davidson-Arnott, 2002).

Bauer and Davidson-Arnott (2002) proposed a framework and derived equations to calculate how the sediment transport rate depends on wind angle, beach geometry (relation between width and length), and fetch effects. For oblique winds, end

effects around, *e.g.*, structures, headlands, river mouths or lagoon inlets, which may limit the fetch upwind or imply that sediment may be lost downwind from the studied stretch of beach, are locally important and can be necessary to consider if the beach length-width ratio is relatively small. As most beaches can be considered to be long relative to their width, end effects will not be considered here.

A few equations exist that describe the spatial growth of sediment transport up to the critical fetch length in agricultural fields (Fryear *and* Saleh 1996; Stout 1990; as cited by Bauer *and* Davidson-Arnott 2002). Those equations assume that the transport, q, develops towards saturated conditions, q_{sat}, according to $q=q_{sat}(1-e^{-kF})$, where F is fetch-length and k an empirical constant.

Precipitation can be a significant limiting factor controlling the fetch length (Bauer *et al.*, 2009). At beaches with seasonal ice and snow cover, the effect on aeolian transport may be significant, especially if the snow and ice cover inhibits the transport during a period with strong winds (Ollerhead *et al.*, 2013).

2.5.4. Sediment budget

Dune build-up by wind requires sediment with a grain size fine enough to be mobilised by the wind, and coarse enough to be deposited in the foredune, where the wind shear stress decreases due to the effect of vegetation and topography (Bauer *et al.*, 2009). Eroding beaches tend to be drained of fine sediment and accreting beaches to be supplied with fine sediment due to the selection of grain size in transport processes, where smaller grains are more likely to be picked up (McLaren and Bowles, 1985).

The beach sediment budget, which could be positive, negative, or stable, affects both the rate of transport and the dune morphology (Psuty, 1988). According to Psuty's conceptual model of sediment budget and beach/dune interactions, four typical dune behaviours can be defined (Figure 2.6). At an accreting beach, dunes will grow fast and create a prograding beach ridge topography, where a new foredune is formed in front of the existing ones, creating low dunes with mild slopes (Hesp, 2002; Psuty, 1988). The dunes are low because there is not enough time for them to grow in height before a new foredune is built in front of them. At a stable beach, the dune stays in place and grows higher due to scarping and recovery (Christiansen and Davidson-Arnott, 2004; Psuty, 1988). Eroding beaches may develop in two different ways, if they are slightly eroding, the dune will maintain or even increase its volume, grow higher, and be displaced inland through scarping in combination with aeolian transport and overwash. If the beach is eroding fast and overwash processes are dominant, the dune will be flattened out and moved landwards.
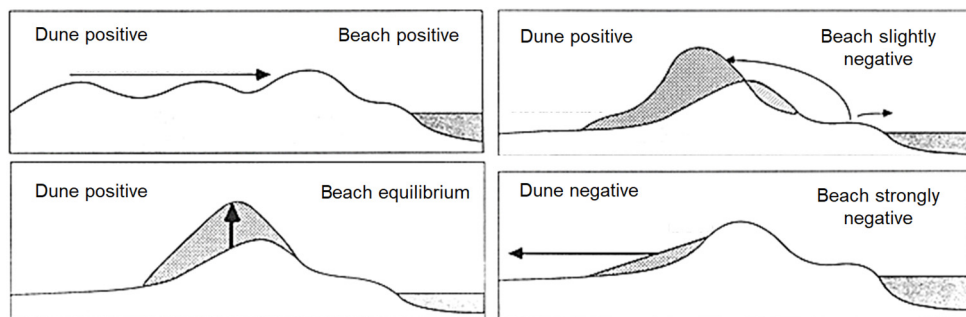
Figure 2.6
Psuty's dune development scenarios for different sediment budgets (modified from Psuty 1988).

In the conceptual model of Psuty (1988) the beach and dune sediment budget are regarded as separate entities. Sherman and Bauer (1993) extended Psuty's conceptual model by adding different steady-states of the beach and dune sediment budget to the existing conditions, creating nine possible combinations of dune and beach budget states. They presented several examples of sites representing the different beach-dune budget conditions, confirming the need for coupling of beach, dune, and nearshore transport processes in coastal evolution models.

The explanatory mechanism behind these different morphological behaviours is sediment supply and the influence of vegetation. If vegetation is present, sediment is trapped in an embryonal foredune and without vegetation sediment is deposited near the foot of the foredune, forming a dune ramp (Figure 2.7), which facilitates the passage of wind-blown sand over the dune crest (Christiansen and Davidson-Arnott, 2004; Kuriyama, Mochizuki, and Nakashima, 2005).

Figure 2.7
Vegetated embryonal foredune (left) at an accreting beach, and non-vegetated dune ramp (right) at a stable beach in Ängelholm, Sweden. Photo: The Author.

36

In a study at Skallingen spit (on the west coast of Denmark), which is a retreating coastal feature subject to overwash and foredune landward migration, the effect of dune ramps was studied (Christiansen and Davidson-Arnott, 2004). After storm erosion had scarped the dunes, part of the eroded sediment was made available for aeolian transport. Aeolian transported sediment formed ramps towards the scarp, which facilitated the wind-blown sand to pass over the crest and deposit on the crest or the landward dune slope. When ramps were well developed, the annual accretion on the landward slope of the foredune amounted to 8–9 m^3 per m beach width, approximately the same volume as stored in the ramps. They observed that aeolian transport over the crest increased rapidly as the vertical distance from the ramp to the crest became equal to or less than 1 m, which could be taken as a critical ramp size. They also observed significant transport over the dune at wet conditions during storms, when there was no transport from the beach to the foredune. This could imply that dune ramp erosion during energetic wind conditions locked the ramp height to approximately that critical height of 1 m below the dune crest (Christiansen and Davidson-Arnott, 2004).

The findings by Christiansen and Davidson-Arnott (2004), of dune translation at transgressive beaches and the influence of ramps, where reconfirmed by a study at Greenwich Dunes on Prince Edward Island in Canada (Ollerhead *et al.*, 2013). Between 2002 and 2009 seasonal and annual sediment deposition were measured along the foredune profile. After scarping, if no ramp was present, minimal sediment reached the dune crest or landward slope. With a dune ramp present, accumulation was observed at the upper seaward slope, crest and landward slope. Vegetated ramps or embryonal foredunes trapped the sediment on the seaward slope so that only small to moderate amounts reached the crest and landward side of the dune. The measurements were performed at two stretches of the beach with different littoral sediment budgets, one negative and one positive or neutral, although both showing a transgressive trend in a long time perspective. The beach with a temporarily positive sediment transport had vegetated embryonal dunes present for 2–3 years and through that time most sediments were deposited at the seaward side of the dune. When the embryonal dune was damaged, and a vegetated ramp had not yet been formed, the observed transport to the crest and landward side of the dune was significant. The profiles from the stretch of the beach with a positive or neutral sediment budget showed 2–4 times greater deposition than the profiles at the stretch of the beach with a negative sediment budget (Ollerhead *et al.*, 2013), indicating that supply is a significant limiting factor for aeolian transport. However, the beaches with higher deposition rates also had a larger beach width, which probably contributed to a higher transport rate. There is no information about grain size variation between the different stretches.

In the Netherlands, different morphological dune developments have been observed at beaches with different nourishment regimes. Nourished beaches show an overall

increase in foredune volume (van der Wal, 2004), whereas dune translation has been observed at a non-nourished beach in the Heemskerk area (Bakker *et al.*, 2012).

For long-term modelling of foredune evolution, dune height is essential as it affects flood safety. The conceptual models of Psuty (1988) and Sherman and Bauer (1993) suggest that dune height is depending on the relation between the beach and the dune sediment budget. Hesp (1988) found a strong relationship between increasing foredune height and increasing dissipativeness but concluded that the trend might also be explained by higher exposure to storm winds at dissipative beaches. Durán and Moore (2013) proposed a linear relationship, based on field data, between foredune height and wave height, assuming that the dune height was depending on wave impact. Van Dijk*,* Arens, and van Boxel (1999) modelled dune evolution with a resulting height/width ratio of 0.11, which they found to be following the upper limit observed in field data. In conclusion, the dune height is site-specific and depends on the sediment budget, wind and wave climate, and sediment and vegetation characteristics.

The sediment budget impacts the supply available for sediment transport. De Vries *et al.* (2014b) found that aeolian transport rates were linearly dependant on wind velocity under supply-limited conditions, as opposed to a cubic relation for abundant supply. They, therefore, suggested that modelling supply is of greater interest than simulating complex wind fields. A field experiment where transport rates were found to vary in time with the tide at constant wind speed supported these theories (de Vries *et al.*, 2014a).

2.5.5. Vegetation

Vegetation is an essential factor for dune growth (Durán and Moore, 2013). The vegetation increases the surface roughness so that the wind speed decreases and sediment more easily deposits. Furthermore, there is a feedback mechanism between the deposition and plant growth as the growth rate of some pioneer species is enhanced by sand deposition (Ranwell, 1972).

If vegetation is present, sediment is trapped in an embryonal foredune, and if no vegetation is present, sediment is deposited near the foot of the foredune (Kuriyama, Mochizuki, and Nakashima, 2005), forming a dune ramp. The embryonal foredune forming around vegetation will eventually build a new dune in front of the other, while the dune ramp is mostly non-vegetated and will form an integral part of the existing foredune and cause bypassing of sediment to the crest and landward side of the dune.

Instead of modelling the vegetation explicitly in a dune model, vegetation can be assumed to be present and accounted for by the sediment budget, following Psuty's

conceptual model. The effect of vegetation would then indirectly be taken into account in the model as accreting beaches are assumed to form embryonal dunes and eroding beaches to form dune ramps. The explanatory mechanism behind the relationship between sediment budget and dune ramps/embryonal foredunes is probably the frequency of runup reaching the dune foot.

Local variation in vegetation cover may have substantial effects on dune evolution and blowouts can significantly impact landward foredune migration (Hesp, 2002), but are difficult to include in numerical models due to their random behaviour and local effect.

3. The CS-model

The CS-model is a semi-empirical model, simulating cross-shore sediment transport and long-term beach and dune evolution. Included processes are dune erosion and overwash, dune build-up by wind, beach-bar exchange, and sea level rise. Gradients in longshore sediment transport are derived from observations or longshore sediment transport models and added as a source or a sink in the model. Nourishments can be implemented at the beach, dune, or foreshore.

In order to resolve all processes at their relevant timescales, the simulation time step should be about 1-3 hours to account for individual storms. Input forcing to the model is wave characteristics, height, period, and direction, simultaneous still water level, wind speed and direction, and sea level rise. The model requires an initial topography of the beach and dune.

The model is based on a set of semi-empirical transport equations, which require site-specific data for calibration and validation. The model is especially sensitive to the empirical coefficients of the dune erosion and aeolian transport equations. Therefore, topographic surveys before and after storms, together with data of long-term dune evolution are crucial to achieve a good model performance.

The model description is based on the work presented in paper I (section 3.1, 3.2, and 3.3), paper V (section 3.1, 3.2, 3.4, 3.5, ad 3.6), and paper VI (section 3.7 and 3.8).

3.1. Profile schematization and sediment balance

The CS-model simulates beach and dune evolution in individual transects, which can be multiple to represent a coastal stretch. The coastal profile is schematized through volumes, exchanging sediment with each other. The shape of the beach and dune is resolved through geometrical equations and is updated in every time step. For the subaqueous part of the profile, an equilibrium profile is assumed (Dean, 1977). The profile schematization in the CS-model is illustrated in Figure 3.1.
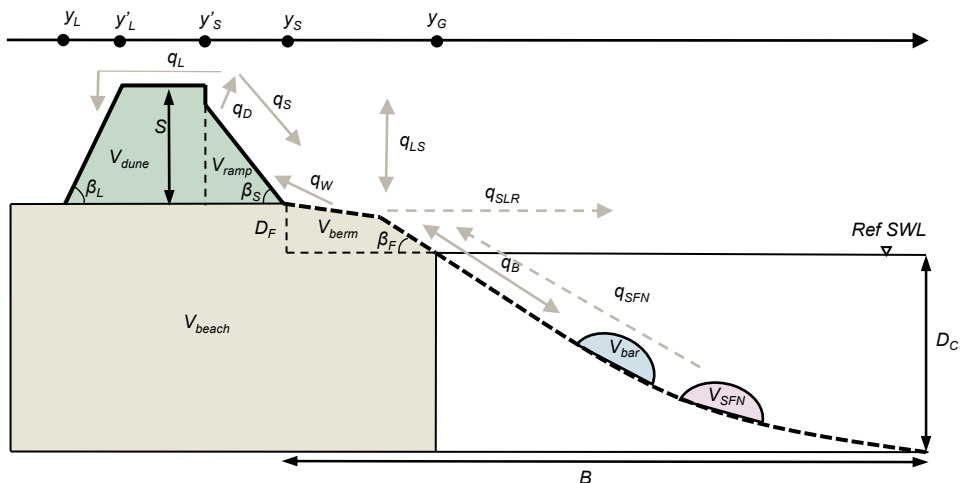
Figure 3.1
Profile schematization; characteristic volumes, heights and angles, length coordinates, and transports.

The dune volume, V_{dune}, is defined as the volume of sediment above the dune foot. The dune foot height, D_F, is given relative to a reference still water level, *SWL*, which can be, *e.g.,* the mean sea level, *MSL*, or the mean low water level, *MLW*. V_{dune} has a subvolume V_{ramp}, which is the volume of a dune ramp. The function of the dune ramp is to control the distribution of aeolian transported sediment across the dune, which is further explained in section 3.5. The slope of the dune ramp is defined by a fixed angle, β_S, taken as the angle of repose of dry sand (approximately 30-34°). The landward dune slope is defined by the fixed angle β_L, which may be derived from observations.

The shape of the dune is defined through the dune crest height, *S*, and four horizontal length coordinates given relative to a reference point behind the dune, y_L and y_S are the landward and seaward dune foot position, respectively, and y'_L and y'_S are the landward and seaward dune crest position, respectively.

The beach volume, V_{beach}, is horizontally limited by a reference point behind the dune and the intersection with the reference *SWL*, y_G; and vertically by D_F and the depth of closure, D_C. The closure depth defines the seaward limit of the active profile. Beyond the closure depth, there is no significant change in bottom elevation and no significant net sediment exchange between the nearshore and offshore (Kraus, Larson, and Wise, 1999). The depth of closure can be calculated from deep-water wave data (Hallermeier, 1978) or multiple measured profiles. The closure depth is a function of the largest waves of a certain duration during the time period considered; the longer timescale, the larger is the value of D_C because the probability of occurrence of more extreme wave events increases with time. Since D_F and D_C

are defined relative to the reference SWL, the elevation of the dune foot and the seaward limit of the active profile, are shifted upwards with SLR.

The beach does not have a specific shape; therefore, the beach profile is represented by a dashed line in Figure 3.1. The beach width is described as a function of a sediment volume, V_{berm}, horizontally limited by y_S and y_G, and vertically by the reference SWL and the dune foot elevation. If a linear relationship is assumed, the beach width is given by,

$$y_G - y_S = aV_{berm} + b \qquad \text{(eq. 3.1)}$$

where a and b are coefficients describing the slope and the intercept with $V_{berm}=0$, respectively.

The rest of the beach volume, V_{beach}-V_{berm} is then given by,

$$V_{beach} - V_{berm} = y_G D_C + y_S D_F \qquad \text{(eq. 3.2)}$$

Through combining equation 3.1 and 3.2 and solving for y_G, the following equation for the intersection with reference SWL is derived,

$$y_G = y_S + \frac{a(V_{beach} - y_S(D_F + D_C)) + b}{1 + aD_C} \qquad \text{(eq. 3.3)}$$

Figure 3.2 displays linear regression of beach width (y_G-y_S) as a function of V_{berm} for observations from the study sites Ängelholm Beach, Sweden and Kennemer dunes, Netherlands.
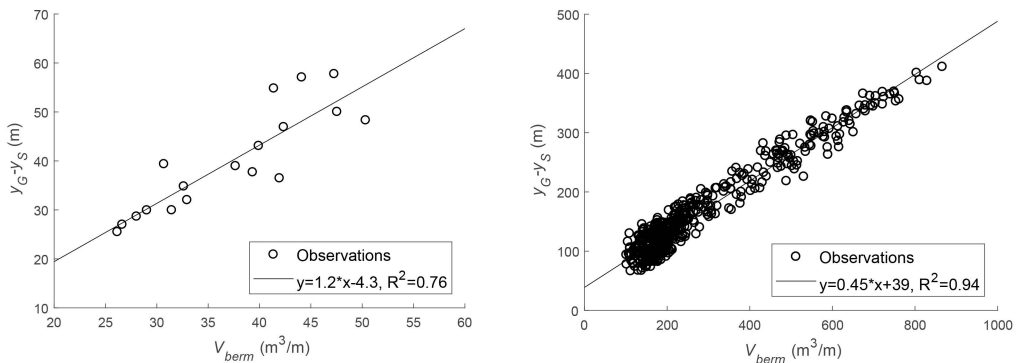
Figure 3.2
Beach width (y_G-y_S) as a linear function of V_{berm} for data from Ängelholm (left panel) and Kennemer dunes (right panel).

The beach width functions presented in Figure 3.2 do not go through the origin, $f(0)\neq0$, which would be expected from a physical point of view; if $V_{berm}=0$ then should $y_G-y_S=0$. However, in a sandy beach and dune system, this condition will never be reached. Therefore, a maximum foreshore slope, β_F, is defined. When the average slope between y_S and y_G is equal to β_F, the entire beach is considered to be part of the swash zone, and the beach cannot erode anymore without eroding the dune. Under this condition, all sediment that would have been eroded from the beach is instead eroded from the dune. Figure 3.3 displays two photographs from beaches under this condition. The left panel displays a beach at the south coast of Sweden (Hagestad) with no astronomical tide at normal water level, and the right panel displays a beach in New Jersey, US (Long Beach Island) at low tide, where the tidal range is about 1.5 m. At the Swedish beach, the waves are reaching the dune toe at normal conditions, and at the US beach, the waves reach the dunes during high tide. The beaches are then constantly wet and the entire beach is subject to swash processes.

Figure 3.3
Hagestad beach (left panel) and Long Beach Island (right panel) at the condition of maximum foreshore slope.
Photo: Caroline Hallin and Björn Almström

V_{bar} is defined as a subaqueous volume that is exchanging sediment with the beach. The sediment can be deposited in one or multiple bars or other nearshore deposits. Sediments added as shoreface nourishments, $V_{nour,SF}$, are in the model stored in a separate volume entity, V_{SFN}. The shape and location of V_{bar} and V_{SFN} are not defined in the model.

Sediment transport is either a source or a sink for the defined volumes. Eroded sediment from the dune, q_D, is either deposited at the beach, q_S, or transported to the landward side of the dune through overwash, q_L. Aeolian transport, q_W, shifts sediment from the beach to the dune. The beach-bar exchange, q_B, is either onshore or offshore directed, depending on the wave climate and volume of sediment in V_{bar}. Gradients in longshore sediment transport, q_{LS}, is either a source or a sink for V_{beach}. Negative longshore transport gradients, *i.e.* accretion is defined as positive q_{LS}, and *vice versa*, $-dQ/dx = q_{LS}$. The offshore directed transport to compensate for sea level

rise, q_{SLR}, is a sink for the beach volume. In the case of shoreface nourishment, there is an onshore transport, q_{SFN}, from V_{SFN} to V_{beach}.

The sediment balance equations for each of the volumes are given by,

$$\frac{dV_{dune}}{dt} = q_W - q_S + \frac{dV_{nour,dune}}{dt} - \frac{1}{2}\left(2y_S - 2y_L - \left(\frac{1}{\tan(\beta_S)} + \frac{1}{\tan(\beta_L)}\right)\Delta S\right)\frac{dS_{SLR}}{dt}$$

(eq. 3.4)

$$\frac{dV_{beach,tot}}{dt} = -q_W + q_S - q_B + q_{SFN} + q_{LS} - q_{SLR} + \frac{dV_{nour,beach}}{dt}$$

(eq. 3.5)

$$\frac{dV_{bar}}{dt} = q_B$$

(eq. 3.6)

$$\frac{dV_{SFN}}{dt} = -q_{SFN} + \frac{dV_{nour,SF}}{dt}$$

(eq. 3.7)

3.2. Dune erosion and overwash

The equations for dune erosion and overwash follow the methods outlined in Larson Erikson, and Hanson (2004) and Larson *et al.* (2009).

Runup height is estimated using the formula (Larson, Erikson, and Hanson, 2004),

$$R = 0.158\sqrt{H_{rms}L_0}$$

(eq. 3.8)

where H_{rms} is the deep-water root-mean-square wave height, and L_0 is the average deep-water wavelength. The runup height is adjusted for friction over the beach according to (Hanson, Larson, and Kraus, 2010),

$$R' = R\exp(-2c_f x_t) + (D_F - SWL)(1 - \exp(-2c_f x_t))$$

(eq. 3.9)

where c_f is an empirical friction coefficient, and x_t is the travel distance of the up-rushing wave. In Hanson, Larson, and Kraus (2010) x_t was defined as the distance from the berm crest to the dune toe over a horizontal berm. Because the profile schematization is different here, the definition of x_t has been modified to,

$$x_t = \frac{2V_{berm}}{D_F}\left(1 - \frac{SWL}{D_F}\right)$$ (eq. 3.10)

Since the beach in the CS-model has no shape, the travel distance cannot be precisely known. Instead, the travel distance is expressed as a function of the volume V_{berm}. In equation 3.10, x_t equals the horizontal distance from the still water line to the dune foot, if V_{berm} has the shape of a right-angled triangle with height D_F.

If the total runup height exceeds the dune foot, $R'+SWL > D_F$, dune erosion will occur, and if the dune crest is exceeded, $R'+SWL > D_F+S$, there will also be overwash. In the case of $D_F < R'+SWL < D_F+S$, the eroded volume from the dune face, q_D, is computed by (Larson, Erikson, and Hanson, 2004),

$$q_D = 4C_S\frac{(R'+SWL-D_F)^2}{T}$$ (eq. 3.11)

where T is the swash period assumed to be equal to the peak period, and C_S is an empirical coefficient, found to be in the range of values $1.7\cdot10^{-4} - 1.4\cdot 10^{-3}$ when calibrated against data from field and laboratory experiments (Larson, Erikson, and Hanson, 2004). All the eroded sediment is deposited on the beach, $q_S = q_D$.

If $R'+SWL > D_F+S$, eq. 3.11 is modified to account for a reduction of the impact force due to the additional momentum flux over the dune (Larson *et al.*, 2009),

$$q_D = 4C_S\frac{(R'+SWL-D_F)S}{T}$$ (eq. 3.12)

A part of the eroded sediment, q_D, will be transported to the landward side of the dune, q_L, and the rest will be deposited on the beach, q_S. Defining $\alpha = q_L/q_S$, then the amount of eroded sediment deposited on the beach and the landward dune slope is described by $q_S = q_D/(1-\alpha)$ and $q_L = q_D \alpha /(1-\alpha)$, respectively. The ratio α is given by (Larson *et al.*, 2009),

$$\alpha = \frac{1}{A}\left(\frac{R'+SWL-D_F}{S} - 1\right)$$ (eq.3.13)

where A is an empirical coefficient determined to be about 3, using field data (Larson *et al.*, 2009).

The volume in the dune ramp, V_{ramp}, is eroded first, the eroded volume is defined as $\Delta V = -q_D \Delta t$, where Δt is the length of the time step. The change of dune foot position is then,

$$\Delta y_S = \frac{\sqrt{2}\left(\sqrt{\tan(\beta_S)(V_{ramp} + \Delta V)} - \sqrt{\tan(\beta_S)V_{ramp}}\right)}{\tan(\beta_S)} \qquad \text{(eq.3.14)}$$

If V_{ramp} has eroded completely so that $y_S = y'_S$, $\Delta y_S = \Delta y'_S$, and $y'_S > y'_L$, then the seaward dune crest will retreat,

$$\Delta y'_S = \frac{\Delta V}{S} \qquad \text{(eq. 3.15)}$$

If also $y'_S = y'_L$ the dune has attained a triangular shape, then $y_S = y'_S = y'_L$ and $\Delta y_S = \Delta y'_S = \Delta y'_L$. Then dune erosion leads to a change of the landward dune crest and the dune height,

$$\Delta y'_L = \frac{\sqrt{\frac{2\Delta V \tan(\beta_L) + S^2}{\tan(\beta_L)^2} \tan(\beta_L)} - S}{\tan(\beta_L)} \qquad \text{(eq. 3.16)}$$

$$\Delta S = \Delta y'_L \tan(\beta_L) \qquad \text{(eq. 3.17)}$$

In the case of overwash, the volume $\Delta V = q_L \Delta t$ is added to the landward dune slope so that,

$$\Delta y'_L = \Delta y_L = \frac{-\Delta V}{S} \qquad \text{(eq. 3.18)}$$

3.3. Beach-bar exchange

The beach-bar exchange of sediment simulates the profile response to changes in wave climate, *i.e.,* summer (berm) and winter (storm) profile. The sediment transport between the beach volume, V_{beach}, and the subaqueous volume, V_{bar} denoted q_B is calculated according to the equilibrium bar volume method proposed by Larson and Kraus (1989),

$$q_B = (V_{bar,eq} - V_{bar})(1 - \exp(-\lambda \Delta t)) / \Delta t \qquad \text{(eq. 3.19)}$$

q_B is a function of the deviation of V_{bar} from an equilibrium bar volume, $V_{bar,eq}$, Δt is the length of the time step. λ is a rate coefficient for offshore directed transport determined by (Larson, Hanson, and Palalane, 2013),

$$\lambda = \lambda_0 \left(\frac{H_0}{wT} \right)^{m_b} \qquad \text{(eq. 3.20)}$$

where λ_0 and m_b are calibration coefficients. Empirical values from calibration against field data are found to be $\lambda_0 = 0.56 \cdot 10^{-6}$ and $m_b = -0.5$ (Larson, Hanson, and Palalane, 2013), for offshore transport. For onshore directed transport, the rate coefficient is estimated to $0.3\,\lambda$, based on field data (Larson, Hanson, and Palalane, 2013).

The equilibrium bar volume depends on the dimensionless fall velocity (the Dean parameter) and wave steepness according to (Larson and Kraus, 1989),

$$\frac{V_{bar,eq}}{L_0^2} = C_B \left(\frac{H_0}{wT} \right)^{4/3} \frac{H_0}{L_0} \qquad \text{(eq. 3.21)}$$

where w is the fall velocity and C_B a dimensionless coefficient.

The change of V_{beach} leads to a change of y_G, which is computed with equation 3.3.

3.4. Aeolian transport

The method to compute aeolian transport is based on the assumption that, on a decadal timescale, the most critical limiting factor for aeolian sediment transport is the supply of material of appropriate grain size. Sediment available for aeolian transport is assumed to be present as a location-specific fraction of the transported sediment volumes longshore and cross-shore. Availability is computed through a balance of sediment transport and nourishments, to and from V_{beach}. The volume of sediment available for aeolian transport, V_W, in time step i is calculated as,

$$V_{W,i} = V_{W,i-1} + (q_{S,i-1} - q_{W,i-1} - A_q(q_{SLR,i-1} - q_{LS,i-1}) + A_S q_{SFN,i-1})\Delta t + A_b V_{nour,i-1}$$

$$V_W \geq 0 \qquad \text{(eq. 3.22)}$$

where V_{nour} is a volume of added artificial nourishment to the beach during the time step. The empirical coefficients A_q, A_S, and A_b describes the fraction of sediment that is exposed to the wind and has the proper grain size for aeolian transport within the specified transport rates and volumes. The aeolian transport is limited by the available sediment, $q_W\Delta t \leq V_W$. If $V_W = 0$ the aeolian transport, q_W, is set to 0. The initially available volume, $V_{W,0}$, depends on conditions prior to the simulation period, *e.g.,* nourishments and large dune erosion events.

The potential aeolian sediment transport rate, m_{WE}, can be calculated with an equilibrium transport formula, *e.g.* the formulation proposed by (Lettau and Lettau, 1978),

$$m_{WE} = K_W \sqrt{\frac{D_{50}}{D_{50}^{ref}}} \rho_a \frac{u_*^2}{g} \left(u_* - u_{*c} \right) \tag{eq. 3.23}$$

where $D_{50}{}^{ref}$ is the median reference grain size (0.25 mm), ρ_a the density of air, g the acceleration due to gravity, u_* the shear velocity at the bed, u_{*c} the critical shear velocity at the bed, and K_W an empirical coefficient. The median grain size, D_{50}, should be chosen as a representative grain size found in the dunes. If $u_* < u_{*c}$, then $m_{WE}=0$.

The shear velocity, u_*, can be calculated using the Prandtl equation, also known as the law of the wall (see, *e.g.* Horikawa 1978),

$$\frac{u_z}{u_*} = \frac{1}{\kappa} \ln\left(\frac{z}{z_0} \right) \tag{eq. 3.24}$$

where u_z is the wind velocity at z meter above ground, z_0 is the aerodynamic roughness height, and κ is von Kármán's constant (≈ 0.41). For the wind velocity conditions below the critical velocity for initiation of transport, the roughness height, z_0, can be parameterised either as $z_0 = D_{50}/30$ (Bagnold, 1941) or $z_0 = 0.081\log_{10}(d/0.18)$ (Zingg, 1953) where d is the grain size in mm, here represented by D_{50}.

The critical shear velocity is calculated from (Bagnold, 1941),

$$u_{*c} = A_W \sqrt{\frac{(\rho_s - \rho_a)}{\rho_a} g D_{50}} \tag{eq.3.25}$$

where A_W is an empirical coefficient equal to 0.1.

The sand movement influences the wind velocity profile through the drag forces of the saltating grains, changing both the slope of the velocity profile and the roughness height. To be able to calculate the shear velocity during transport, two wind measurement at different heights or one measurement and an estimate of the roughness height under transport conditions are required. For long-term simulations, wind data is typically not available from the beach of interest but from a wind gauge nearby, from which the measurements are not affected by the aeolian sand transport.

In order to relate the wind speed at the gauge to the shear velocity at the beach, the relationship between u_z and u_* can be approximated as linear (Belly, 1964). Following equation 3.23, $m_{WE} \propto u_z^2(u_z - u_{z,c})$ (Fryberger and Dean, 1979). The critical velocity for transport at z m height, $u_{z,c}$ can be computed by combining equation 3.24 and 3.25. Equation 3.23 can then be rewritten as,

$$m_{WE} = C_W \sqrt{\frac{D_{50}}{D_{50}^{ref}}} \rho_a \frac{u_z^2}{g}(u_z - u_{zc})$$ (eq.3.26)

where C_W is an empirical coefficient.

The mass flux m_{WE} is converted to a volumetric equilibrium transport rate, q_{WE}, of sand to the dunes by,

$$q_{WE} = \frac{m_{WE}}{\rho_s(1-P)}$$ (eq. 3.27)

where ρ_s is the density of sand (typically 2,650 kg/m³) and P the porosity (typically 40%).

In order to reach the transport rates described by the equilibrium equations, a critical fetch length is required (Bauer *et al.*, 2009; Davidson-Arnott and Law, 1990). The fetch length, F, depends on the wind angle towards shore normal, θ, and the dry beach width, B_{dry}. Aeolian transport due to offshore directed wind is neglected. For values of θ up to 80°,

$$F = \frac{B_{dry}}{\cos(\theta)}$$ (eq. 3.28)

The dry beach width, B_{dry}, is calculated as the horizontal distance from the runup limit, y_R, to the seaward dune foot, $B_{dry} = y_R - y_S$. If $y_R \leq y_S$, the whole beach is assumed to be wet and there will be no aeolian transport from the beach to the dune.
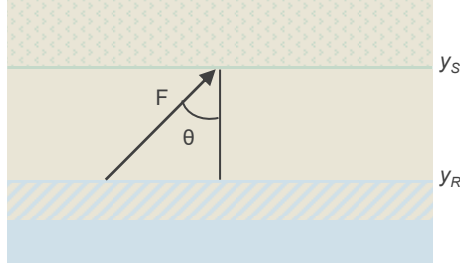
Figure 3.4
Definition of fetch length and wind angle.

The runup limit y_R is computed assuming a constant slope from y_G to y_S by,

$$y_R = y_S + \left(1 - \frac{R + SWL}{D_F}\right)\left(y_G - y_S\right) \qquad \text{(eq. 3.29)}$$

A simplified equation for the potential transport rate, corrected for fetch-limited conditions, q_{WF}, was developed based on the work by Sauermann, Kroy, and Herrmann (2001),

$$q_{WF} = q_{WE}\left(1 - \exp\left(-\delta F\right)\right) \qquad \text{(eq. 3.30)}$$

where δ is an empirical coefficient in the order of 0.1–0.2 m^{-1}, which should be representative of the wind conditions where most aeolian sediment transport occurs. Eq. 3.30 has the same form as the equation derived for aeolian transport in agricultural environments by Stout (1990) and Fryear and Saleh (1996).

Oblique wind angles have longer fetches and may, therefore, generate higher aeolian transport rates. However, only the onshore component, q_W, adds to the dune volume,

$$q_W = q_{WF} \cos(\theta) \qquad \text{(eq. 3.31)}$$

Precipitation is not included in the model but may be an important factor controlling the fetch length (Bauer *et al.*, 2009). At beaches with seasonal ice and snow cover, the effect on aeolian transport may be significant, especially if the transport is inhibited during periods with strong winds (Ollerhead *et al.*, 2013). In areas with a significant impact of rain, snow, and ice, sediment availability in the model could be modified during wet or frozen conditions to restrict aeolian transport.

3.5. Morphological dune evolution

Dunes will evolve differently depending on where the aeolian transported sediment is deposited, in front of the dune, on the seaward slope, on the crest, or on the landward slope. The sediment deposition scheme is based on the sediment budget formulation by Psuty (1988) and the dune ramp concept described by Christiansen and Davidson-Arnott (2004).

The sediment budget is calculated as the change of volume in the beach-dune system, ΔV_T, over a significant timescale, T_{bud}, and can either be negative, $\Delta V_T < 0$, stable, $\Delta V_T \approx 0$, or positive, $\Delta V_T > 0$:

$$\Delta V_T = \frac{1}{n}\sum_{t=i-n}^{t=i}\left((-q_{SLR,t}+q_{LS,t})\Delta t + V_{nour,t}\right) \qquad \text{(eq.3.32)}$$

where $n = T_{bud}/\Delta t$ and V_{nour} nourished volumes to the dune, beach or foreshore. The significant timescale, T_{bud}, is in the order of years and should be long enough to represent long-term trends and not seasonal variations. The distribution scheme generates different dune evolution depending on the sediment budget, which is illustrated in Figure 3.5.
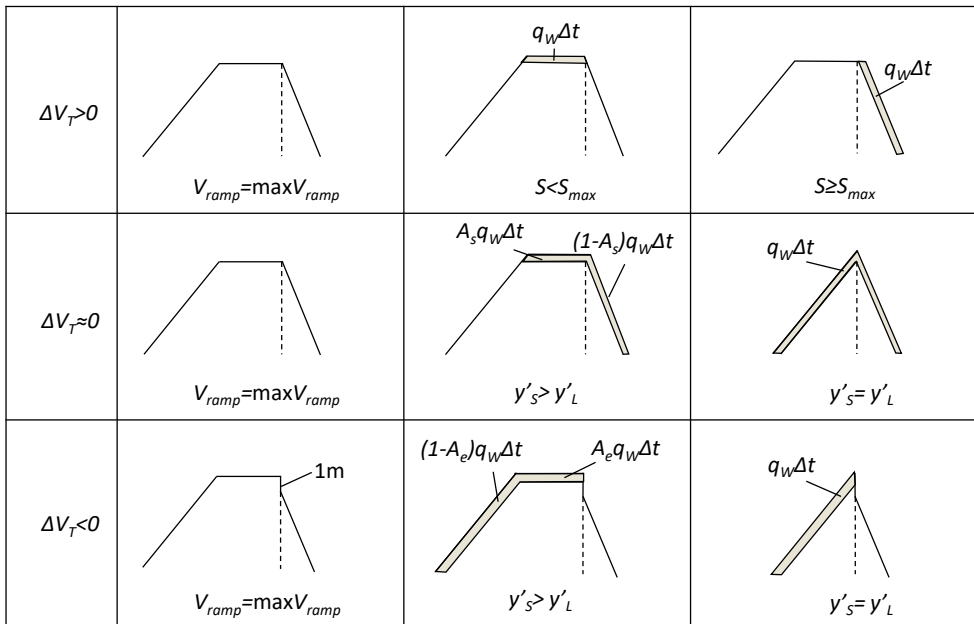
Figure 3.5
Sediment distribution scheme of wind-blown sand on a dune depending on sediment budget, ΔV_T.

In the case of a positive sediment budget, $\Delta V_T > 0$, the ramp is filled until the ramp height is equal to the dune height, S. After the ramp has filled up, if $S < S_{max}$, for a trapezoidal shape, the sediment will be deposited on the crest. If the dune has a triangular shape, the dune grows symmetrically in its place, maintaining a constant dune crest coordinate, $y'_L = y'_S =$ constant, until S_{max} is reached. If $S \geq S_{max}$, all sediment is deposited on the seaward side of the dune and the dune grows seaward maintaining a trapezoidal shape.

For a stable sediment budget, $\Delta V_T \approx 0$, the ramp is filled until the ramp height is equal to the dune height, S. Thereafter, in the case of a trapezoidal dune shape, a fraction of the sediment, A_s, is deposited on the crest and the fraction $1-A_s$ is deposited on the seaward side of the dune. If the dune has a triangular shape, the dune grows symmetrically in its place, maintaining a constant dune crest coordinate, $y'_L = y'_S =$ constant.

When the sediment budget is negative, $\Delta V_T < 0$, the ramp is filled until a critical ramp height is reached. Thereafter, in the case of a trapezoidal dune shape, a fraction of the sediment, A_e, is deposited on the crest and the fraction $1 - A_e$ is deposited on the landward side of the dune. If the dune has a triangular shape, $y'_L = y'_S$, the dune grows on its landward side.

In a field study at Skallingen spit in Denmark, Christiansen and Davidson-Arnott (2004) observed that aeolian transport over the dune crest increased rapidly as the vertical distance from the top of the ramp to the crest became equal to or less than 1 m, and that the wind during wet conditions eroded the ramp to approximately this height. Based on their findings the critical ramp height is here defined as 1 m below the crest level. If the model is applied in an area where local observations suggest differently, a site-specific value of the critical ramp height should be adopted. The distribution coefficients, A_s and A_e, are also assumed to be site-specific and may be derived from observations. If no observations are available, both parameters can be assumed to be 0.5 based on the observations by Ollerhead *et al.* (2013).

The evolution of dune shape parameters for $\Delta V = q_W \Delta t$ is derived from geometrical relationships. If $V_{ramp} < V_{ramp,max}$ the seaward dune foot is changed according to equation 3.14.

3.5.1. Positive sediment budget equations

If the sediment budget is positive, $\Delta V_T > 0$, the following equations describe the change of affected dune shape parameters.

If $S < S_{max}$ and the dune has a triangular shape, $y'_S = y'_L$,

$$\Delta S = \sqrt{\frac{(y_S - y_L)S + 2\Delta V}{\frac{1}{\tan(\beta_S)} + \frac{1}{\tan(\beta_L)}}} - S \qquad \text{(eq. 3.33)}$$

$$\Delta y_S = \frac{\Delta S}{\tan(\beta_S)} \qquad \text{(eq. 3.34)}$$

$$\Delta y_L = -\frac{\Delta S}{\tan(\beta_L)} \qquad \text{(eq. 3.35)}$$

If $S < S_{max}$ and the dune has a trapezoidal shape, $y'_S > y'_L$,

$$\Delta S = \frac{\sqrt{-2\left(\left(-\frac{1}{2}(y'_L - y'_S)^2 \tan(\beta_S) + \Delta V\right)\tan(\beta_L) + \tan(\beta_S)\Delta V\right)\tan(\beta_S)\tan(\beta_L) + (y'_L - y'_S)\tan(\beta_S)\tan(\beta_L)}}{\tan(\beta_S) + \tan(\beta_L)}$$

$$\text{(eq. 3.36)}$$

$$\Delta y'_S = -\frac{\Delta S}{\tan(\beta_S)} \qquad \text{(eq. 3.37)}$$

$$\Delta y'_L = \frac{\Delta S}{\tan(\beta_L)} \qquad \text{(eq. 3.38)}$$

If $S \geq S_{max}$ and the dune has a trapezoidal shape, $y'_S > y'_L$,

$$\Delta y'_S = \Delta y_S = \frac{\Delta V}{S} \qquad \text{(eq. 3.39)}$$

3.5.2. Stable sediment budget equations

If the sediment budget is stable, $\Delta V_T \approx 0$, the following equations describe the change of affected dune shape parameters.

If the dune has a trapezoidal shape, $y'_S > y'_L$,

$$\Delta S = \frac{y'_S - y'_L}{\frac{1}{\tan(\beta_S)} + \frac{1}{\tan(\beta_L)}} - \sqrt{\frac{(y'_S - y'_L)^2}{\left(\frac{1}{\tan(\beta_S)} + \frac{1}{\tan(\beta_L)}\right)^2} - \frac{2A_S\Delta V}{\frac{1}{\tan(\beta_S)} + \frac{1}{\tan(\beta_L)}}}$$

$$\text{(eq. 3.40)}$$

$$\Delta y'_S = -\frac{\Delta S}{\tan(\beta_S)} + \frac{(1-A_S)\Delta V}{S+\Delta S} \qquad \text{(eq. 3.41)}$$

$$\Delta y_S = \Delta y'_S + \frac{\Delta S}{\tan(\beta_S)} \qquad \text{(eq. 3.42)}$$

$\Delta y'_L$ is defined by eq. 3.38.

If the dune has a triangular shape, $y'_S = y'_L$, ΔS, Δy_S, and Δy_L are defined according to equation 3.33 – 3.35.

3.5.3. Negative sediment budget equations

If the sediment budget is negative, $\Delta V_T < 0$, the following equations describe the change of affected dune shape parameters.

If the dune has a trapezoidal shape, $y'_S > y'_L$,

$$\Delta S = \tan(\beta_L)\left(y'_S - y'_L - \sqrt{(y'_S - y'_L)^2 - \frac{2A_e\Delta V}{\tan(\beta_L)}} \right) \qquad \text{(eq. 3.43)}$$

$$\Delta y'_L = \frac{\Delta S}{\tan(\beta_L)} - \frac{(1-A_e)\Delta V}{S+\Delta S}$$
$$\text{(eq. 3.44)}$$

$$\Delta y_L = -\frac{(1-A_e)\Delta V}{S+\Delta S} \qquad \text{(eq. 3.45)}$$

If the dune has a triangular shape, $y'_S = y'_L$,

$$\Delta S = \sqrt{\tan(\beta_L)S(y'_L - y_L) + 2\Delta V} - S \qquad \text{(eq. 3.46)}$$

Δy_L is defined according to equation 3.38.

3.6. Sea level rise

The Bruun Rule concept is used to calculate the required sediment transport from the beach volume, V_{beach}, to the active part of the profile to compensate for SLR. In agreement with Rosati, Dean, and Walton (2013), also landward transport is accounted for to compensate for an elevation adjustment of the dry beach (Figure 3.6). Analogous to the original Bruun Rule concept, the dry beach is assumed to be subject to hydrodynamic forcing capable of adjusting it to a slowly rising sea level. The explanatory mechanism is that the beach is built by waves, with a higher MSL, the waves will build a higher beach. Therefore, the width of the active profile, B, is here extended to encompass the horizontal distance from the seaward dune foot, y_S, to the depth of closure, D_C.
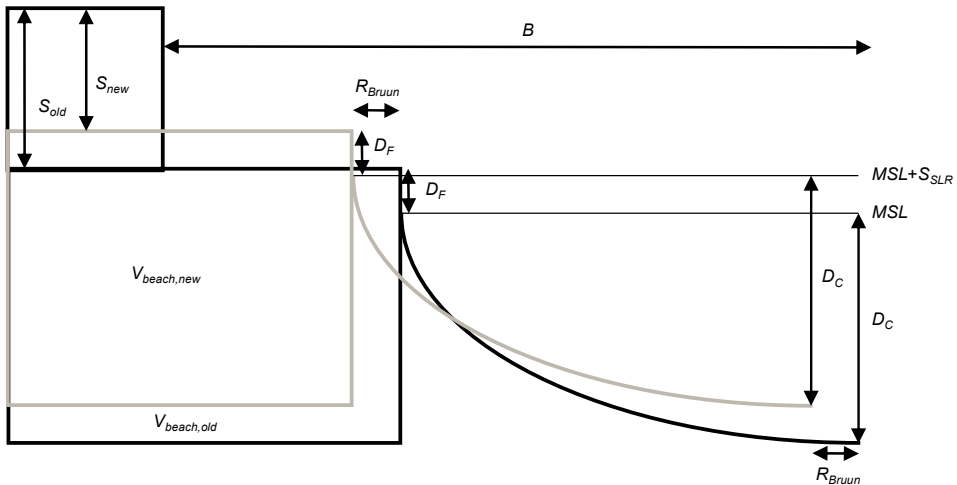
Figure 3.6
Impact of sea level rise on beach volume and dune height. The beach and dune volumes are for simplicity of the visualisation schematized as rectangular shapes.

The dune foot height is assumed to be kept constant relative to MSL. When the beach moves up with SLR, the dune height decreases and part of the dune volume, V_{dune}, is converted to beach volume, V_{beach}. The difference between the old and new V_{beach} is denoted V_{SLR}. Thus, the volume V_{SLR} is eroded from the beach. V_{SLR} is derived from the modified Bruun Rule,

$$V_{SLR} = R_{Bruun}(D_F + D_C) = S_{SLR}B \qquad \text{(eq. 3.47)}$$

The sediment transport required to maintain the equilibrium profile, q_{SLR}, is taken as the time derivative of V_{SLR},

$$q_{SLR} = \frac{dV_{SLR}}{dt} = \frac{dS_{SLR}}{dt} B \qquad \text{(eq. 3.48)}$$

Consequently, there are two direct effects of SLR in the CS-model: first, adjustment of the equilibrium profile to the new sea level by an offshore Bruun Rule transport, q_{SLR}, from the beach volume V_{beach}. Second, decrease of dune volume, V_{dune}, and height, S, due to an upward shift of the reference SWL through $\Delta S = S_{SLR}$, $\Delta y_L = S_{SLR}/\tan(\beta_L)$, and if $y_S > y'_S$, $\Delta y_S = -S_{SLR}/\tan(\beta_S)$.

The aeolian transport and morphological dune evolution scheme are indirectly impacted through q_{SLR} (equation 3.22 and 3.32). Furthermore, the Bruun Rule transport is a sink for the beach volume, which will reduce wave energy dissipation over the beach (equation 3.9 and 3.10) and thus increase the probability of dune erosion and overwash.

3.7. Longshore transport gradients

Gradients in longshore sediment transport is a cause of beach erosion and accretion. In the CS-model, longshore transport gradients are converted to a source or sink term for the beach profile, q_{LS}, with the units $m^3/m/s$, $q_{LS} = -dQ/dx$. The gradients in longshore transport can be derived either from data or longshore transport models, such as Unibest CL+ and GENESIS. Work is currently undertaken to couple the CS-model to Unibest CL+ to be able to resolve temporal and spatial variations in longshore sediment transport and to include the feedback from cross-shore processes on longshore transport mechanisms.

3.8. Nourishments

Nourishments can be added to the beach, dune, or shoreface. In the case of beach nourishment, the nourished volume V_{nour} is added to V_{beach}, and the morphology is updated according to equation 3.3. Dune nourishments are by default added to the front of the dune. First, the dune ramp is filled up according to equation 3.14, and then the dune grows seaward according to equation 3.39.

To account for shoreface nourishment, a nearshore volume, V_{SFN}, has been introduced, to which the shoreface nourishments are added. From V_{SFN} sediment

migrate onshore, adding to V_{beach}. The onshore transport rate, q_{SFN}, is computed with a relationship identical to the beach-bar exchange equation (equation 3.19) but with the equilibrium volume set to zero and a new calibration coefficient, K_{SFN}, introduced,

$$q_{SFN} = (V_{SFN})(1 - \exp(-K_{SFN}\lambda\Delta t))/\Delta t \qquad \text{(eq. 3.49)}$$

The coefficient K_{SFN} is calibrated to a value between 0 and 1, meaning a slower response of the nourished volume to wave impact compared to beach-bar exchange, which is in accordance with data from outer bars located in larger water depths (Larson, Hanson, and Palalane, 2013). The response coefficient λ is a function of the Dean parameter, (equation 3.20) leading to an increase in onshore transport for larger waves.

This approach was developed in the Kennemer Dunes study (paper V) and fitted well to the observed behaviour of the shoreface nourishments in the study area, where the beach responded to the shoreface nourishments with a time lag. Furthermore, the method is compatible with the model concept and assumption of an equilibrium profile in the subaqueous region. However, the suggested method is not generally applicable and should be used with care since the behaviour of shoreface nourishments varies with the setting, placement, and size (van Duin *et al.*, 2004).

4. Study sites

Long-term beach and dune evolution has been analysed from data and simulated with the CS-model at two study sites; Ängelholm Beach in Sweden (paper II, III, IV, and V) and the Kennemer Dunes in the Netherlands (paper VI).

4.1. Ängelholm Beach, Sweden

Ängelholm Beach is located in Skälderviken Bay in southwestern Sweden (Figure 4.1). The beach is situated between two small rivers, the Rönne River in the north and the Vege River in the south. The beach has a sheltered location in the bay but is almost yearly impacted by storm surges and large waves from the northwest, causing beach and dune erosion.
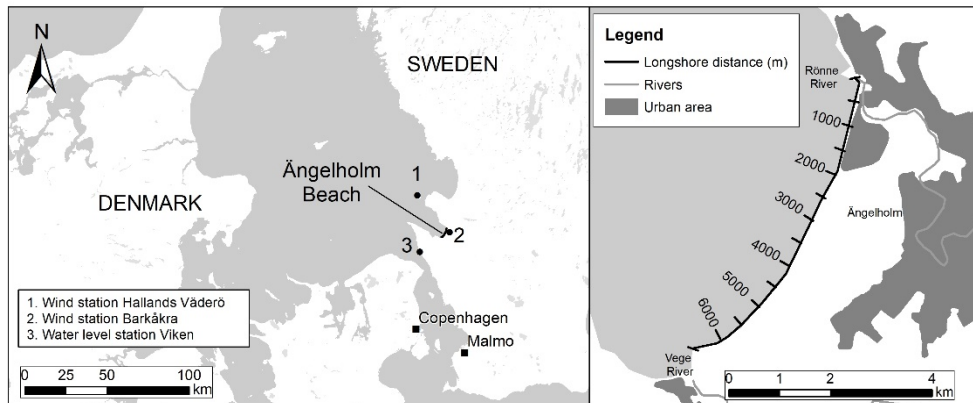
Figure 4.1
Maps of the study area Ängelholm Beach. The left panel shows the location of the study area and the right panel shows Ängelholm Beach, where the longshore distance, x, is marked along the beach.

For the study, topographic observations have been available from 2010 to 2017 and aerial photos from the 1940s, 1960s, 2000s, and 2010s.

Water levels have been measured in Viken by SMHI (Swedish Meteorological and Hydrologic Institute) since 1976 (station 3; Figure 4.1). Wind data was compiled

for the same period (station 1 and 2; Figure 4.1) and used to compute an offshore wave climate at the bay mouth (Figure 4.2), using a modified version of the SMB-method (Hanson and Larson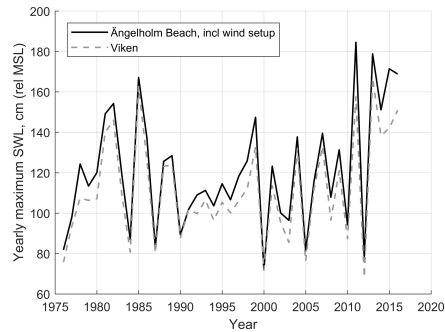, 2008; USACE, 1984). The largest computed significant wave height and peak period are 5.3 m and 9.3 s, respectively, which occurred on 06/12/2013.
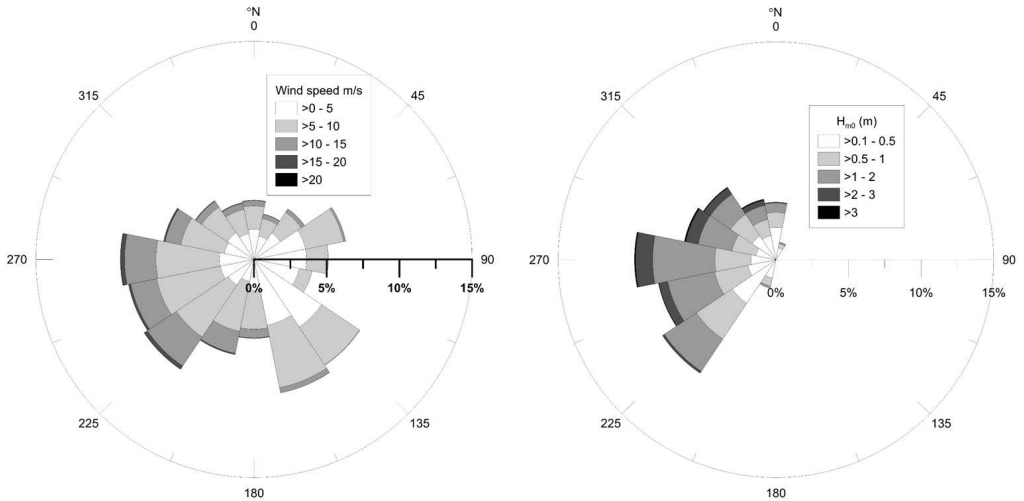
Figure 4.2
Wind rose compiled with data from 1976–2016 (left panel) and hindcasted spectral significant wave heights offshore for the same period (right panel) at Ängelholm Beach.

Figure 4.3
Yearly maximum SWL in 1976-2016 based on measurements from Viken, which have been corrected for the local wind setup in Skälderviken Bay.

Figure 4.3 shows the yearly maximum still water levels (SWL) corrected for wind setup in the bay. During the last decade, multiple storms have occurred (2011, 2013, 2014, 2015 and 2016) that caused higher storm surges than in the previous two decades.
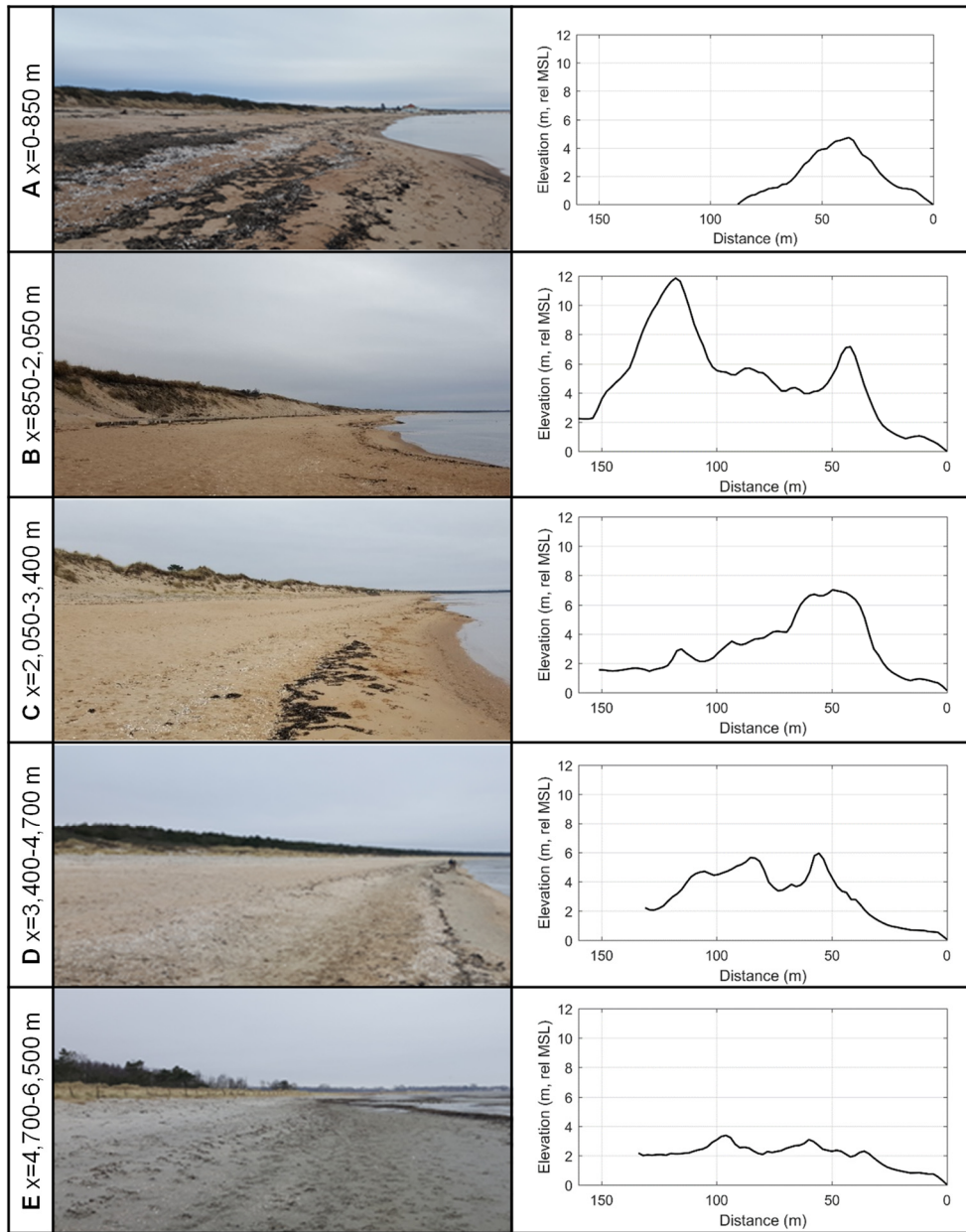
Figure 4.4
Characteristic beach and dune profiles in section A-E, the longshore distance *x*, refers to the scale presented in Figure 4.1. Dune profiles in the right panels are extracted from the National DEM, the distance on the x-axis is relative the intersection with MSL. Photo: Caroline Hallin

The beach has been divided into five sections (Figure 4.4) based on dune morphology and defined by their longshore distance from the mouth of Rönne River (Figure 4.1). Figure 4.4 shows photos from the different sections together with typical cross-sections of the dune and dry beach, extracted from the Swedish National Elevation Model from 2010.

In the northern part of the beach, Section A, the outlet of Rönne River is stabilized with 380 m long jetty. The dune height, defined from the dune foot to the foredune crest, is about 2–4 m in this area. After a storm in 1967, the dunes were reconstructed with a gabion core (Almström and Fredriksson, 2011). In 2000, the beach and dunes were nourished with 53,000 m^3 of sand taken from the north side of the harbour jetties at the outlet.

Further south in Section B, the dunes are higher (5–6.5 m high) and have been eroding in multiple storms during the last decade. After the storms in 2011, 2013, 2014, 2015, and 2016, the dunes have been replenished with sediment from the surf zone in the following spring. At some of these occasions, also the dunes within Section A were replenished.

In Section C, the dune erosion has not been as severe, and the dunes have to a larger extent recovered after storm events due to aeolian processes. The dunes are about 4-5 m high.

Further south, in Section D, the beach is wider, and dunes are lower, 2–4 m. The dune system consists of multiple dune rows. In section E, the dunes are only about a 1–1.5 m high and the beach is wide, low-lying, and moist. In these two southernmost sections, the beach erosion has been much less severe than in the northern part, except for an area within section D, where the dune vegetation has been removed in a habitat restoration project (Lindell, Fredriksson, and Hanson, 2017).

The colour of the beach is changing from more red in the north (Section A), where the sand has a larger content of feldspar, towards more white in the south (Section E), where quartz is dominant.

The profiles referred to as Profile A, B, and C in paper II and V are located within section B, C, and D, respectively.

4.2. Kennemer Dunes, Netherlands

The Kennemer dunes are located south of IJmuiden Harbour on the Holland coast in the Netherlands (Figure 4.4). IJmuiden harbour was constructed in the mid-19th century to provide access to the port of Amsterdam. In 1965, the harbour jetties were

extended; the north jetty to a length of 2 km and the south jetty to 2.5 km (Luijendijk *et al.*, 2011). After this extension, significant accretion took place at the south breakwater, and the beach started to erode further south (van Rijn, 1997). The eroding stretch of the beach has thereafter been subject to multiple nourishment projects. The locations and years of the nourishments within the study period are indicated in Figure 4.5.
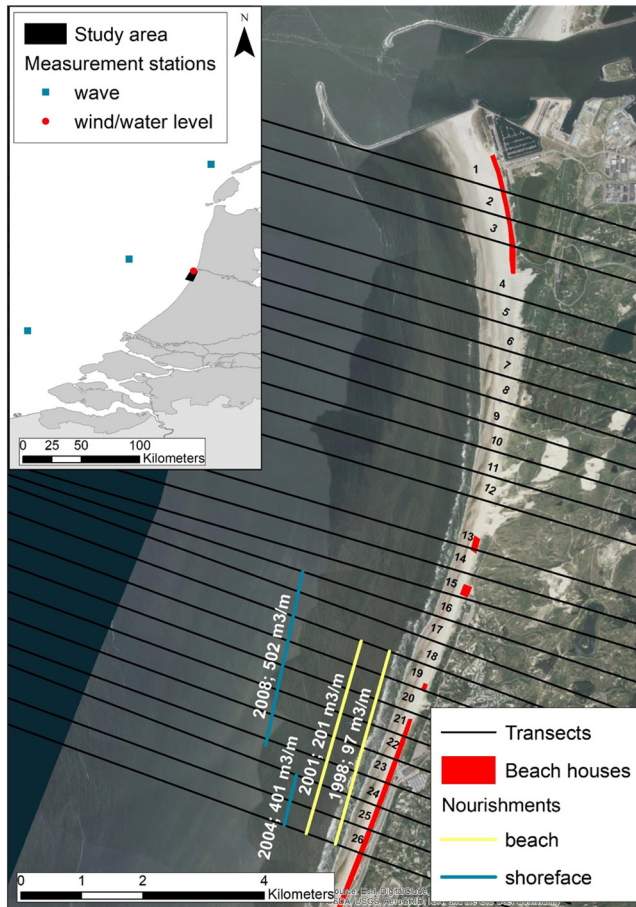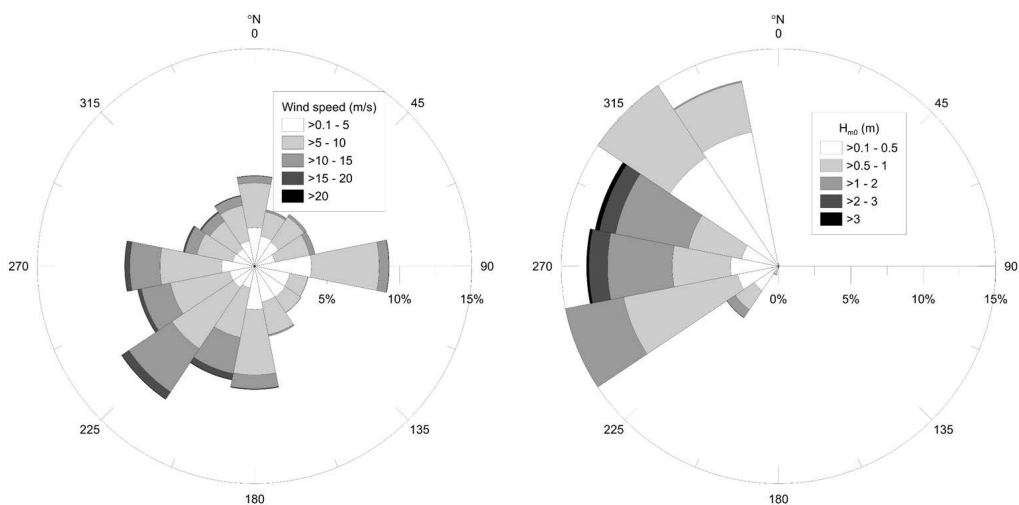

Figure 4.5
Maps of the study area Kennemer dunes, measurement stations, nourishments and location of beach houses.

For this study, a 22-year long data set, from 1994 to 2016, with topographic and bathymetric data (profile 1-26, indicated in Figure 4.5) from JARKUS (Rijkswaterstaat, 2017), in combination with wind, water level, and deep-water wave observations were available.

The average tidal range is about 1.6 m with a maximum of 1.9 m (Wijnberg, 2002). The mean low water level is -0.8 m relative MSL. During the winter season storm surges occur and the highest observed total still water level (SWL) within the time series was +3.06 m relative MSL at 11/9/2007.

The wind climate is dominated by winds from SSW to W (Figure 4.6). The wind data together with measured deep-water significant wave height, period, and direction were used to simulate the nearshore wave climate at 8 m depth using the SWAN wave model (Booij, Ris, and Holthuijsen, 1999). The wave climate is dominated by waves from WSW to WNW (Figure 4.6). The average wave height during the simulation period is 0.8 m and the maximum 3.3 m. The average peak wave period is 4.6 s and the maximum about 14 s.

Figure 4.6
Wind rose compiled with data from 1994-2016 (left panel) and simulated spectral significant wave heights at 8 m depth in profile 12 for the same period (right panel) at the Kennemer dunes.

In profiles 1–3, 13–15, and 18–26, temporary buildings, so-called beach houses, are placed on the beach during summer time (Figure 4.5). The foredunes in these profiles are moulded into terraces before placement of multiple rows of beach houses. Figure 4.6 displays photographs of moulded and freely evolving dunes from a field visit in September 2017, when the beach houses had recently been removed.

Figure 4.7
Beach house terraces in profile 3 (left panel) and freely developing foredunes in profile 9 (right panel). Photo: The Author

There is significant variability in dune shape and beach width alongshore. Figure 4.8 displays profile evolution from 1995 to 2005 with a five-year interval, for selected profiles. Beach widths are largest in the northernmost profiles and decrease in the southward direction. The wider beach in the northern profiles is the result of the blockage of longshore sediment transport by the IJmuiden harbour. Profiles 18-26 would have had an eroding trend during the study period if it were not for the contribution of the nourishments.
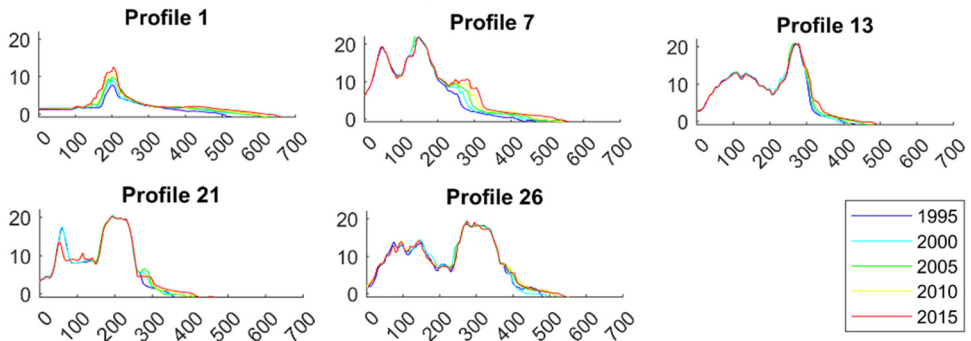
Figure 4.8
Subaerial part of profiles (> -0.8 m relative MSL) from north to south (increasing numbers) at Kennemer dunes (Jarkus dataset). Length and height units are meters.

The dunes in profiles 1–3, closest to the harbour jetty are low and grow in height during the study period. They are part of a new dune row formed in front of the constructed lake Kennemermeer. The other profiles are part of one coherent dune landscape with an elevation of about 20 m above MSL. Profiles 4–12, which do not have temporary buildings in front of them, show fast accretion rates in the

foredunes. Profiles 4 and 5 grow at slightly lower rates than the adjacent profiles, which could be related to an opening in the dunes between profiles 3 and 4 (can be seen as a sandy area in Figure 4.5) functioning as a sediment sink.

5. Model application

This chapter presents selected results from the model applications in the appended papers. The chapter starts by describing the results of the investigation of the relationship between grain size sorting and transport processes at Ängelholm Beach. After that, the results from the long-term CS-model simulations of beach and dune evolution at Ängelholm Beach are presented for a range of SLR scenarios. In the last section, model sensitivity and the relation between dune evolution and sediment supply from different transport processes are presented for the case study at the Kennemer Dunes.

The results and discussion are based on the work presented in paper III and IV (section 5.1), V (section 5.1 and 5.2), and VI (section 5.3).

5.1. Sediment availability - Ängelholm

A fundamental assumption for dune build-up in the CS-model is that the availability of sediment in the appropriate grain size is limiting aeolian transport. The interaction between transport processes and grain size was studied based on a data set from Ängelholm Beach consisting of 308 sediment samples distributed alongshore and cross-shore in five transects. The cross-shore distributed samples were collected on 12/10/2015, 22/04/2016, 21/09/2016, 27/10/2016, and 19/12/2018; however, not all transects and not all sampling points were sampled on each occasion. The long-shore distributed samples, 58 samples with 110 m spacing, were collected on 28/03/2018 and 19/12/2018. The longshore distributed samples were taken from the mid-beach face position half-way between the swash zone and wrack line or berm crest, known as the Bascom reference point (Bascom, 1951). The Bascom reference point is located between sampling point 1 and 2 indicated in Figure 5.2.

The result of the grain size sampling alongshore on 28/03/2018 is presented in Figure 5.1. The upper left panel displays the distribution of D_{50}. There are two peaks around 0.15 mm and 0.30-0.35 mm, which could be explained by wind erosion in the sample point since grain sizes between 0.15 and 0.30 mm are most easily entrained by the wind (Bagnold, 1941).

The median grain size is correlated with five variables, in the order of the strongest correlation: longshore distance ($R^2 = 0.69$), average H_S ($R^2 = 0.57$), observed change of vegetation line ($R^2 = 0.51$), observed change of shoreline ($R^2 = 0.32$), and computed gradients in longshore transport, dQ/dx, ($R^2 = 0.17$). It should be noted that all the investigated parameters co-vary. The strong correlation with longshore distance is explained by a nearly unidirectional longshore sediment transport from north to south.
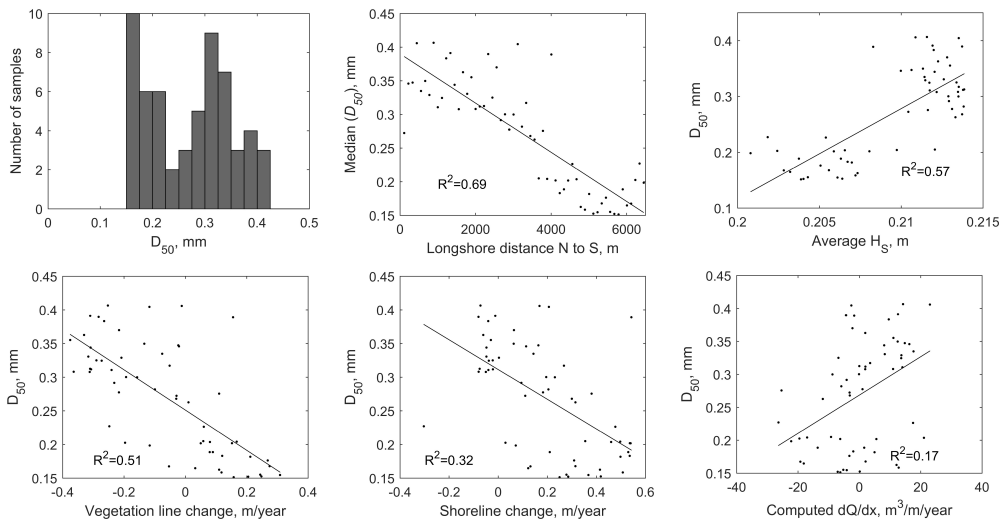
Figure 5.1
Distribution of D_{50} and correlation with longshore distance, average significant wave height, observed vegetation line change, observed shoreline change, and computed gradients in longshore transport (dQ/dx). The samples were collected on 28/03/2018.

The relation between grain size and vegetation line change indicates that the parts of the beach where $D_{50} > 0.3$ mm show a long-term negative development, *i.e.,* erosion, whereas a positive development is observed for parts where $D_{50} < 0.3$ mm.

The results of the cross-shore sampling during the simulation period for the three profiles that are modelled in paper V are presented in Figure 5.2. The profiles A, B, and C, have different long-term beach and dune evolution behaviour. Profile A at $x = 1450$ m has a long-term eroding trend, profile B at $x = 3050$ m has been stable, and profile C, at $x = 4050$ m has been accreting. Profiles A, B, and C are located within section B, C, and D, respectively (Figure 4.4).

The grain size found in sample point number seven is assumed to be representative for dune building sediment. In profile B and C, the median grain size in the dune is about 0.2–0.3 mm, whereas in profile C it is finer, 0.1–0.15 mm. These fine sediments originate from dune nourishments with a silty material; they have not

been transported from the beach by the wind. Thus, the median grain size of dune building material in the area is assumed to be within 0.2–0.3 mm.

The results show that sediment availability is variable in space and time (Figure 5.2). In profile A, sediments of the dune-building grain size, about 0.2–0.3 mm, are only available in a couple of the samples from the first sampling occasions. In profile B, these sediments are intermittently available in the three most nearshore sample points. In profile C, these sediments are available at most sampling occasions; but on the first sampling occasion, the sediments found in the four most nearshore samples were finer than the dune-building sediment.
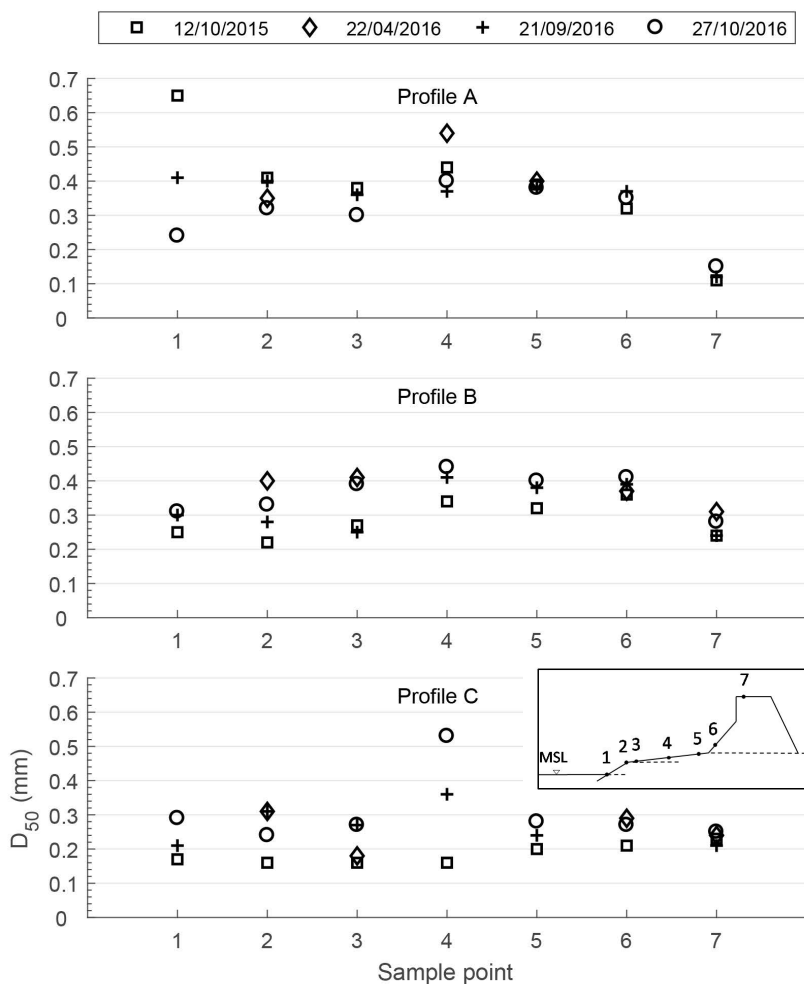
Figure 5.2
Median grain size, D_{50}, for sediment samples from the shoreline (1) to the dune crest (7) in cross-shore transects located at the longshore distance x=1450 m (Profile A), x=3050 m (Profile B), and x=4050 m (Profile C) from the Rönne's mouth.

The CS-model was used to simulate beach and dune evolution at Ängelholm Beach, during 2010–2017. Available sediment for aeolian transport in the berm and aeolian transported volumes for the period are displayed in Figure 5.3. The rapid increases of sediment availability, which can be seen as almost vertical changes in the left panel, are due to dune erosion. In profile A, the increases are followed by a decrease when sediment has been excavated from the surf zone to nourish the dune.
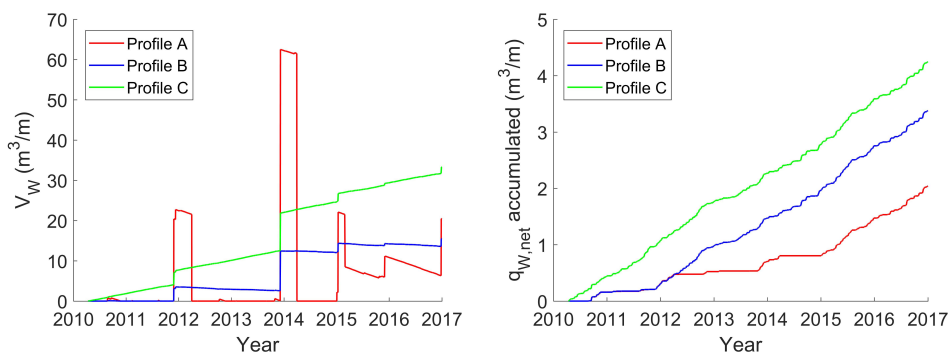
Figure 5.3
Available sediment for aeolian transport, V_W, and accumulated aeolian transport, q_W, in CS-model simulations.

The simulation results, with the highest aeolian transport in profile C and lower transport in profile A, are in line with the topographic observations. The simulated differences in the average annual transport rates are due to variations in sediment supply between the different profiles as well as the variation in beach width. The four sets of sediment samples taken from October 2015 to October 2016 display variations both in space and time (Figure 5.2). This pattern is reflected in the simulated available sediment (Figure 5.3), where profile C has the most available sediment, profile B less, and profile A only intermittent availability during the period 2010–2016. However, the simulation results show that there should be sediment available for aeolian transport within all three profiles during the actual sampling period, which was not supported by the sediment grain size data (Figure 5.2). An explanation for this could be that the material eroded from the dune in profile A before the sampling period was finer than the appropriate grain size for dune build up, due to the silty nourishment, and thus should not have been accounted for in the available sediment volume, V_W.

In summary, topography and grain size data suggest that the dune evolution at Ängelholm Beach conforms to the morphological concepts in the CS-model. The different profile characteristics fit the conceptual model by Psuty (1988), where the eroding and stable dunes in profiles A and B are the highest and the accumulating profile C displays a lower, prograding dune-ridge topography. The differences in

the distribution of D_{50} over the profiles are in line with the assumption that available sediment is an important controlling factor for aeolian transport and that preconditions for aeolian transport are variable both in space and time.

5.2. Long-term evolution with climate change - Ängelholm

The CS-model was used to simulate the long-term beach and dune evolution at Ängelholm Beach for a range of SLR scenarios from 2018–2100. The simulations were run with ten sets of input data, obtained by randomly shuffling years with input data from 1976 – 2016. Three different IPCC scenarios of SLR until 2100 (Church *et al.*, 2013) were compared to a no change scenario. The first scenario "mean low" corresponds to the mean of the RCP 2.6 scenario with SLR of 0.44 m, relative to the average MSL during the years 1986–2005. The second and third scenario, "mean high" and "upper high" corresponds to the mean and likely upper range of the RCP 8.5 scenario with SLR of 0.74 m and 0.98 m, respectively. The regional climate change prognosis does not predict any significant changes to the wind climate (Persson *et al.*, 2012); therefore no changes in wind speed or direction were considered in this study. The same holds for the wave climate, which is dominated by regionally wind-generated waves.

Profile A was simulated with two different values on the dune erosion impact coefficient, C_S; a calibrated value of $5 \cdot 10^{-4}$, which partly is assumed to be affected by the dune nourishments during the calibration period, and a lower value of $7.5 \cdot 10^{-5}$, which was estimated for profiles B and C.

In all profiles, dune volumes decrease for all three scenarios (Figure 5.4). In Profile A, the dune erodes completely before the end of the simulation period in the year 2100, both with the large and small dune erosion coefficient, C_S. In the simulations with large C_S, dune erosion is more important than the effect of SLR; also without SLR, the dune is eroded quickly. For profile B, the dune only disappears completely in the upper high SLR scenario, but the volume is markedly diminished also in the other two scenarios. In Profile C, the effect of SLR is compensated by the positive gradient in the longshore transport, which is added as a constant transport rate to the beach volume. Still, the long-term simulation without SLR does not show a net dune growth which could be expected on an accreting beach. This behaviour can be explained by the severe storm events in 2011 and 2013 that are present in the data set. If the wind climate from 1976 – 2016 is representative for future conditions, the model results indicate that the aeolian transport capacity will not be sufficient to repair storm erosion and compensate for dune volume losses due to SLR effects.
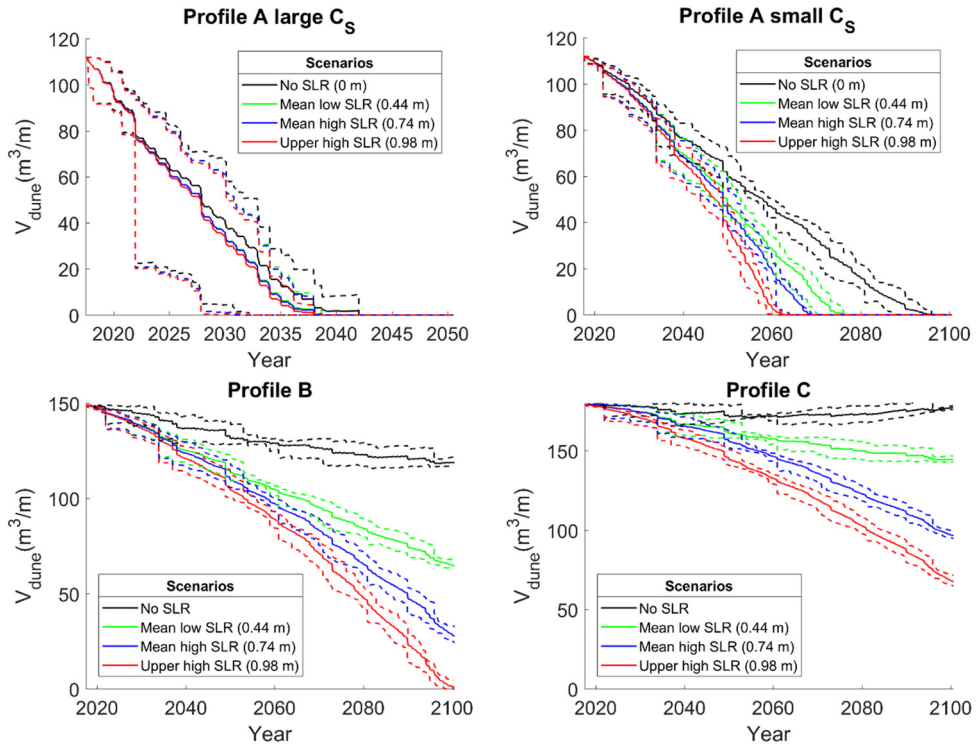
Figure 5.4
Simulated dune volume evolution. Solid lines represent mean value, and the dashed lines represent min and max values from the ten simulations for each scenario.

In profiles B and C, the available sediment for aeolian transport is accumulating faster than the aeolian transport rate, the gradient in longshore transport causes the beach volume to increase and the shoreline to extend seawards (Figure 5.5). The wider beach increases frictional losses, so that dune erosion decreases which explains the trend change in dune volume evolution in profile C for the low and baseline scenarios in Figure 5.4.

The dunes are losing sediment due to the change of reference dune foot elevation when the sea level is rising, causing the dune crest height to decrease (Figure 5.5). In profile B, with no gradient in the longshore transport, SLR changes the sediment budget from stable to eroding for all scenarios. Profile C is still accreting in the low scenario but changes into a negative sediment budget in the mean high and upper high scenarios. None of the simulations of profile B and C results in landward dune translation. In the scenarios with negative sediment budget, the aeolian transport capacity is too low to restore the dune ramp, which is supposed to produce landward translation between consecutive erosion events.

72
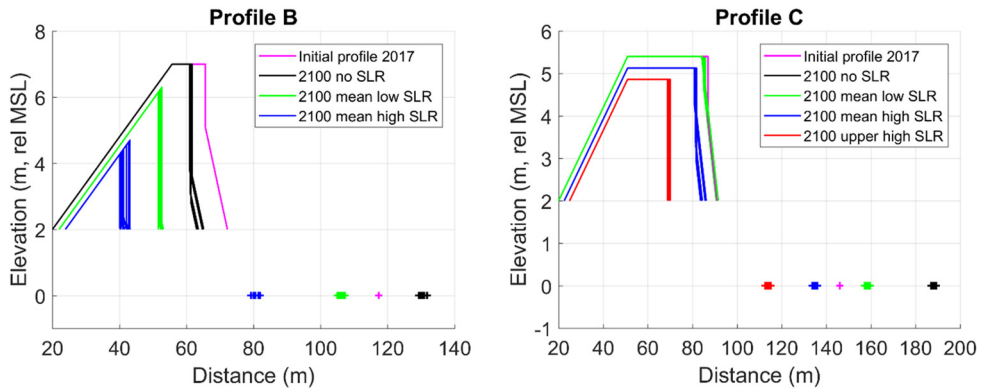
Figure 5.5
Simulated beach–dune evolution for Profile B and C. The '+' indicates intersection with MSL.

The results suggest that for the long-term evolution with SLR at Ängelholm Beach, both the aeolian transport capacity and the sediment availability limit the dune growth. Thus, if the wind climate remains unchanged compared to the period 1976-2016, interventions, such as beach and dune nourishment, will be needed to maintain the dunes. In profile A where the dunes protect the hinterland from flooding, interventions are required within the coming decades.

5.3. Sediment supply and dune evolution - Kennemer

The CS-model was used to investigate the impact of different transport processes, and interventions, on sediment supply and dune evolution 1994 to 2016 for the Kennemer Dunes. The combined results from the calibration (1994–2010) and validation (2011–2016) periods are displayed in Figure 5.6. Overall, the simulations show a satisfactory agreement with the observations for most of the profiles. The dune evolution behaviour showed a large variety within the study area – the total dune growth during the simulation period varies by an order of magnitude. The model still managed to reproduce this variability, using the same values on the calibration parameters for all profiles, which were mainly based on values from the literature.
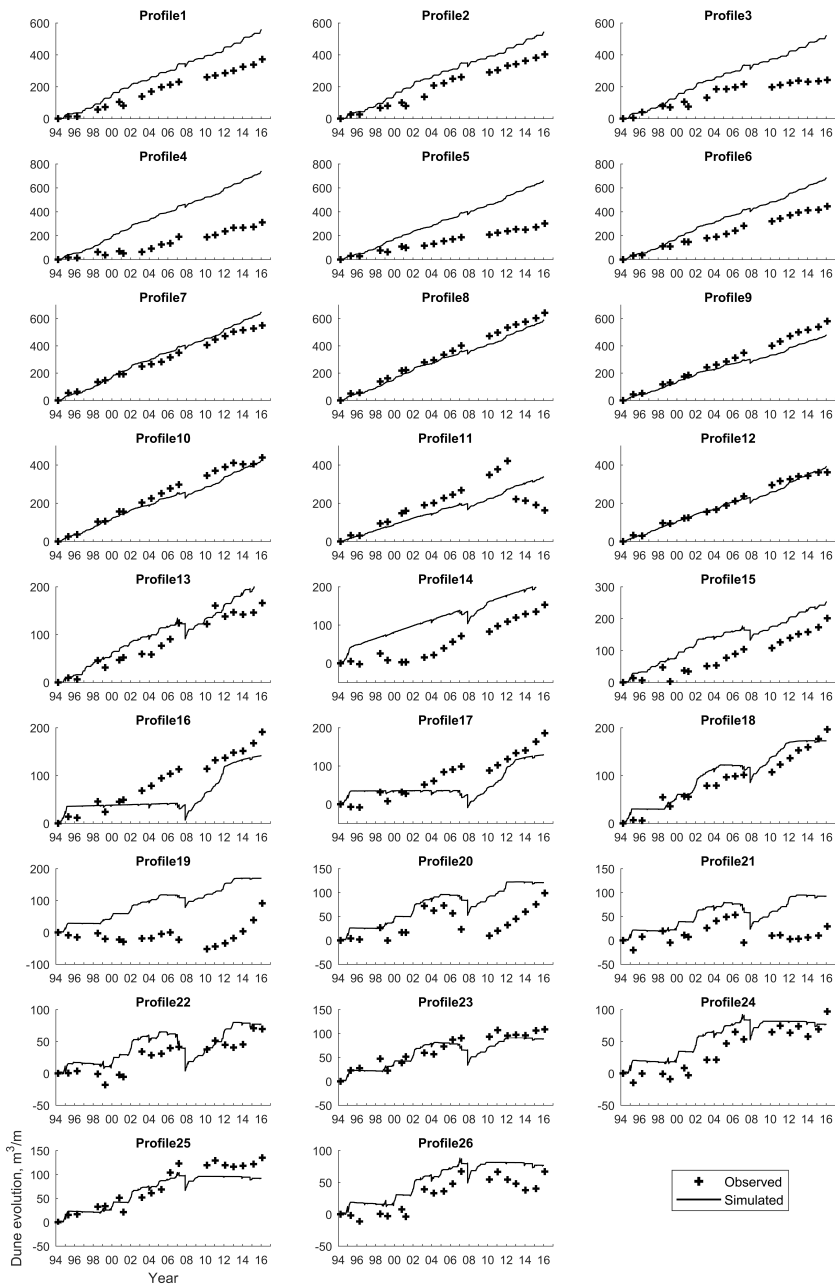
Figure 5.6
Simulated and observed dune volume evolution from 1994-2016 at the Kennemer Dunes.

In the accreting ($q_{LS} > 0$) profiles 1–15, the modelled and observed dune volume evolution show overall good agreement. For the most northern profiles 1–6, dune growth is, however, over-predicted, which can partly be explained by the opening in the dunes between profiles 3 and 4 (Figure 4.5) that functions as a sediment sink for wind-blown sand moving alongshore. Furthermore, the grain size is expected to be finer in the sheltered area next to the harbour jetties, which would also lead to decreased aeolian transport if capillary forces keep the beach wet; however, there are no data available to validate these assumptions.

In profile 11 the simulation results deviate from the observations in 2012–2016, where the simulation shows continued dune growth while erosion is observed. In the adjacent profiles 10, 12, and 13, decreased dune growth is observed for this period compared to previous years. This behaviour is explained by vegetation removal as a part of a restoration project, which can be observed as sandy areas in the dunes in Figure 4.5 (Ruessink *et al.*, 2018). In profiles 13 and 15, which have seasonal beach houses, dune growth is well predicted, suggesting that the influence of beach houses is relevant to consider

Profiles 16–26 show alternating periods with accretion, stagnation, and erosion of the dune volume. The southern-most profiles, 18–26, would have been eroding as a result of longshore transport gradients ($q_{LS} < 0$), but the nourishments counteracted the erosion. The connection between nourishments and dune growth is clearly shown by the stepwise dune evolution, with enhanced dune growth after the placement of the nourishments.

In profiles 21–26 observed dune growth reduced considerably from 2012 onwards, both in the simulations and the observations. The simulation results for profiles 18–20 also show reduced dune growth, whereas observations show continued accretion. Longshore spreading of nourished sediment from the more southern transects, which is not included in the model, could explain the deviation between simulations and observations.

In order to assess the relative contribution from different transport processes, the dune evolution was simulated while excluding specific processes. The most important model components for the long-term dune evolution was found to be the longshore transport gradients and nourishments because of their impact on sediment availability for aeolian transport. The second most important processes were the dune erosion and the blocking of aeolian transport due to beach houses. The beach-bar exchange and sea level rise had a small impact on the dune evolution in the study area during the investigated period.

Results from three profiles are displayed in Figure 5.7: profile 2 – an accreting profile ($q_{LS} > 0$) with beach houses; profile 7 – an accreting profile without beach

houses; and profile 23–an eroding profile ($q_{LS} < 0$) with beach houses that was subject to nourishments in 1998, 2001, and 2008.
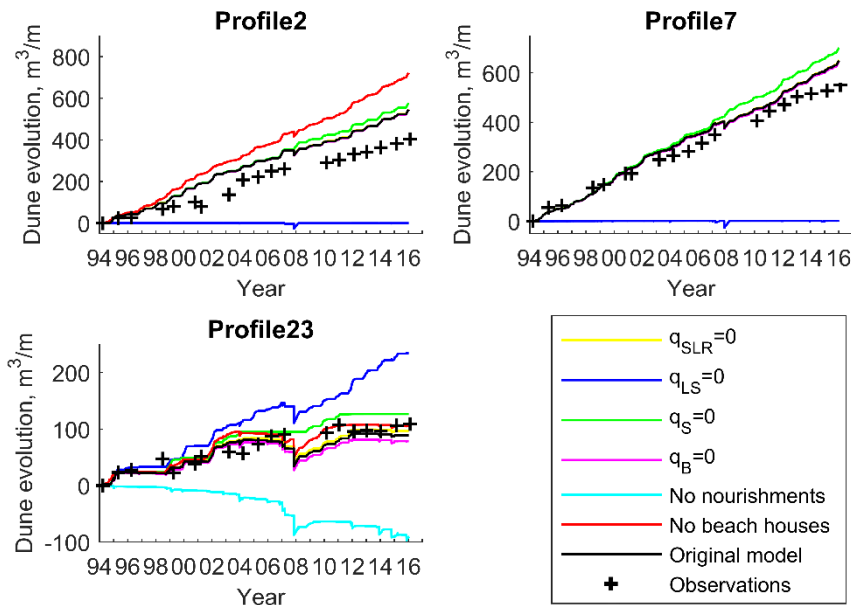
Figure 5.7
Simulations of dune evolution with different processes excluded from the original model from three profiles at Kennemer Dunes; q_{SLR} is a Bruun-type transport to compensate SLR, q_{LS} is gradients in longshore transport, q_S is dune erosion, and q_B is beach-bar exchange.

In profiles 2 and 7, supply from longshore transport is the primary source of sediment for aeolian transport. When dune evolution is simulated without gradients in longshore transport (the blue line in Figure 5.7), dune growth only occurs when sediment has been made available through dune erosion. In profile 23, for which nourishments are the primary source of sediment for aeolian transport, the dune growth is overestimated, if the longshore transport gradients are neglected. This overestimation is because the aeolian transport depends on the volume of available sediment, which in profile 23 is depleted by longshore transport.

If nourishments are excluded (the cyan line), the dune in profile 23 erodes with almost 100 m^3/m during the simulation period. The dune recovers partly after the major storm event in 2007, but the long-term dune evolution is negative since the beach erodes. If dune erosion is not considered (the green line), the dune growth is overestimated in all profiles.

The impact of beach houses was investigated by assuming that no beach houses are present in any profiles (the red line). Compared to the original model (the black line), the dune growth is then overestimated in profiles 2 and 23.

In summary, the results demonstrate that longshore transport gradients are a crucial factor for long-term dune evolution at the Kennemer Dunes. In beach profiles with long-term erosion, nourishments were found to have a significant impact on dune evolution through supplying sediment for aeolian transport. The aeolian transport increased after the nourishments, both in simulations and observations, which is in agreement with previous observations along the Dutch coast (Bakker *et al.*, 2012).

The studies at Kennemer Dunes and Ängelholm beach have shown that the CS-model can be used to analyse how the relative importance of different transport processes vary with location and time. In the future, the importance of sea level rise is expected to increase as the sea level rise accelerates. The simulation results from Kennemer Dunes suggest that the CS-model could be a useful tool to evaluate different coastal management strategies through, *e.g.,* analysing the impact of nourishment and beach houses.

6. Conclusions and future work

In this thesis work, a numerical model (the CS-model) for simulating decadal to centennial-scale beach and dune evolution has been developed and tested. The CS-model is a semi-empirical cross-shore sediment transport model that includes dune erosion and overwash, beach-bar exchange, dune build-up through aeolian transport, and beach erosion and accretion due to gradients in longshore transport. Methods to simulate the aeolian transport and morphological dune evolution were developed from established geomorphological concepts, which were translated into numerical formulations. Sediment supply was found to be an important controlling factor for the aeolian sediment transport. A sediment balance equation for sediment supply was developed based on theories of sediment sorting, which were tested against data on grain-size distribution from Ängelholm Beach.

The CS-model was applied to two study sites, Ängelholm Beach in Sweden and the Kennemer Dunes in the Netherlands. In Ängelholm, the model was calibrated and validated against a seven-year long data set and the long-term beach and dune evolution from 2017 – 2100 was simulated for a range of sea level rise scenarios. At Kennemer Dunes, the model was applied to a 22-year data set, to study the relative importance of different transport processes for the long-term dune evolution. At Ängelholm Beach, dune erosion was found to be a dominant process for the long-term dune evolution, because the aeolian transport capacity was limited. At Kennemer Dunes, the gradients in longshore sediment transport were governing the dune volume evolution. The simulations also showed that the beach and shoreface nourishments were the most critical factors for dune growth along the long-term eroding stretches of the beach.

The scientific contribution of the thesis is primarily the capability to simulate long-term dune evolution, considering the effects of erosion by waves and sea level rise as well as build-up by wind. The model applications at the study sites have contributed to increased understanding of the local coastal processes, especially at Ängelholm Beach where the coastal processes have not previously been investigated at this level of detail. The investigation of grain-size variability and the relation to transport processes has provided valuable insights for the concept of sediment availability in aeolian transport models. The results also provide useful knowledge to promote dune growth in design of nourishment projects.

The CS-model is designed to be fast and robust, which makes it suitable for probabilistic long-term simulations for a range of future scenarios. The results are promising and suggest that the model could be a useful tool for long-term coastal risk assessment and evaluation of coastal management strategies. However, there are parts of the model that need further development, and to fully validate the numerical implementation of the proposed morphological concepts, applications of the model to more extensive and detailed data sets are needed.

The sediment distribution scheme based on the conceptual model by Psuty (1988) needs to be validated against an extensive high-resolution data set. The spatial and temporal resolution of topographic data should be sufficient to study the mechanism of dune ramp development, and include eroding, stable, and accreting coastal stretches. Furthermore, the model should be tested at beaches with different types of dune vegetation. So far, it has only been tested in environments dominated by marram grass (*Ammophila arenaria*) and lyme grass (*Leymus arenarius*). The type of vegetation is expected to impact the morphological evolution of the dunes and could be accounted for by tuning the empirical coefficients in the sediment distribution scheme.

The proposed schematization of the beach width, y_G-y_S, as a function of the beach volume, V_{berm}, is a useful concept in this type of profile evolution models, without a cross-shore grid. In the case studies, a simple linear equation was sufficient to describe the relationship, since the maximum foreshore slope angle, β_F, limits the beach width for small beach volumes. However, from a physical perspective, this description is unsatisfactory, as the equations did not go through the origin; if the volume is zero, the width should also be zero. It would be worthwhile to investigate the relationship between beach width and volume in a more extensive data set, from multiple beaches, to develop a more generic, physics-based concept.

In the current configuration of the CS-model, longshore transport gradients are derived from historical data. Changes to the longshore transport due to varied forcing conditions or shoreline orientation are then difficult to reproduce. Work is currently undertaken to couple the CS-model to Unibest CL+, a one-line type coastal evolution model. The idea is to exchange longshore sediment transport gradients and shoreline evolution between the models. With such a coupling, temporal and spatial variations in longshore sediment transport could be resolved, and feedback from cross-shore processes on longshore transport mechanisms could be simulated. A coupled model will allow a more holistic representation of the beach and dune system at spatial scales of kilometres, which is desirable from a coastal management perspective.

Already in its present form, the CS-model is capable of simulating long-term beach and dune evolution with satisfactory results. The combination of subaqueous and subaerial transport processes in long-term simulations is a much-needed

contribution to the existing suite of coastal evolution models. The CS-model fills this gap and yet, based on the schematized representation of morphological units and their interaction, can represent morphological evolution over decades in time and kilometres in space.

List of symbols

A	Empirical coefficient in the equation to determine α
a	Slope coefficient in the linear beach width function $[m^{-1}]$
A_b	Coefficient describing fraction of nourishments available for aeolian transport [-]
A_e	Coefficient describing fraction of sediment deposited on dune crest in a negative sediment budget [-]
A_q	Coefficient describing fraction of longshore and Bruun Rule transport available for aeolian transport [-]
A_s	Coefficient describing fraction of sediment deposited on dune crest in a stable sediment budget [-]
A_W	Coefficient in critical shear velocity equation [-]
B	Width of active profile [m]
b	Coefficient describing the intercept with $V_{berm}=0$ in the linear beach width function [m]
B_{Bruun}	Width of active profile in the original Bruun rule [m]
B_{dry}	Dry beach width [m]
C_B	Calibration coefficient for equilibrium bar volume [-]
c_f	Empirical friction coefficient for wave runup [-]
C_S	Dune erosion impact coefficient [-]
C_W	Empirical coefficient in aeolian equilibrium transport formula [-]
d	Grain size [mm]
D_{50}	Median grain size [mm]
D_{50}^{ref}	Median reference grain size [mm]
D_C	Depth of closure [m]
D_F	Dune foot height [m]

F	Fetch (aeolian transport) [m]
g	Standard acceleration due to gravity [m/s^2]
H	Deep-water wave height [m]
h	Height of active profile [m]
H_{m0}	Energy based significant wave height [m]
H_{rms}	Deep water root-mean-square wave height [m]
H_s	Significant wave height [m]
i	Index, time step [-]
K_{SFN}	Rate coefficient for onshore transport from shoreface nourishments [-]
K_W	Empirical coefficient in aeolian equilibrium transport formula [-]
L_0	Mean deep water wave length [m]
m_b	Calibration coefficient for beach-bar exchange [-]
MLW	Mean low water level [m]
MSL	Mean sea level [m]
m_{WE}	Potential aeolian transport rate [kg/s/m]
n	Number of timesteps [-]
P	Porosity [-]
Q	Longshore transport rate [m^3/s]
q_B	Transport rate between the beach and the bar [m^3/s/m]
q_D	Transport rate of eroded sediment from the dune [m^3/s/m]
q_L	Transport rate of eroded sediment from the dune front to the landward side of the dune [m^3/s/m]
q_{LS}	Transport rate due to gradients in longshore transport [m^3/s/m]
q_S	Transport rate of eroded sediment from the dune to the beach [m^3/s/m]
q_{SFN}	Onshore transport from shoreface nourishments [m^3/s/m]
q_{SLR}	Transport rate of sediment to compensate for sea level rise, 'Bruun Rule' transport [m^3/s/m]
q_W	Onshore component of aeolian transport [m^3/s/m]

q_{WE}	Potential aeolian transport rate [m^3/s/m]
q_{WF}	Potential aeolian transport rate corrected for fetch length [m^3/s/m]
R	Runup [m]
R'	Runup corrected for friction over beach [m]
R^2	Coefficient of determination [-]
R_{Bruun}	Shoreline retreat due to sea level rise [m]
S	Dune height [m]
S_{max}	Maximum dune height limiting vertical dune growth for positive sediment budget [m]
S_{new}	Dune height after SLR [m]
S_{old}	Dune height before SLR [m]
S_{SLR}	Height of sea level rise [m]
SLR	Sea level rise [-]
SWL	Still water level [m]
t	Time step [-]
T	Wave period [s]
T_{bud}	Significant timescale for sediment budget [s]
u_*	Shear velocity [m/s]
u_{*c}	Critical shear velocity [m/s]
u_z	Wind speed at z m elevation [m/s]
$u_{z,c}$	Critical wind speed at z m elevation [m/s]
V_{bar}	Volume of subaqueous deposits [m^3/m]
$V_{bar,eq}$	Equilibrium bar volume [m^3/m]
V_{beach}	Total beach volume [m^3/m]
V_{berm}	Volume of beach above mean sea level, between shoreline and dune foot [m^3/m]
$V_{beach,new}$	Total beach volume after SLR [m^3/m]
$V_{beach,old}$	Total beach volume before SLR [m^3/m]
V_{dune}	Dune volume [m^3/m]

V_{nour}	Nourishment volume [m³/m]
$V_{nour,beach}$	Nourishment volume of beach nourishment [m³/m]
$V_{nour,dune}$	Nourishment volume of dune nourishment [m³/m]
$V_{nour,SF}$	Nourishment volume of shoreface nourishment [m³/m]
V_{ramp}	Dune ramp volume [m³/m]
$V_{ramp,max}$	Maximum dune ramp volume [m³/m]
V_{SFN}	Volume of shoreface nourishment [m³/m]
V_{SLR}	Eroded volume from V_{beach}, due to SLR [m³/m]
V_w	Volume of sediment available for aeolian transport [m³/m]
w	Fall velocity [m/s]
x	Longshore distance [m]
x_t	Horizontal travel distance of wave front [m]
y'_L	Landward dune crest length coordinate [m]
y'_S	Seaward dune crest length coordinate [m]
y_G	Shoreline length coordinate [m]
y_L	Landward dune foot length coordinate [m]
y_R	Runup limit length coordinate [m]
y_S	Seaward dune foot length coordinate [m]
z	Wind gauge elevation [m]
z_0	Roughness height [m]
α	Ratio between landward and seaward transport during overwash events
β_F	Maximum foreshore slope angle [°]
β_L	Landward dune slope angle [°]
β_S	Seaward dune slope angle [°]
δ	Empirical coefficient to account for fetch effect [m⁻¹]
ΔV_T	Change of volume in beach- dune system to determine sediment budget [m³/m]

κ	von Karman's constant [-]
λ	Rate coefficient for beach-bar exchange [-]
λ_0	Calibration coefficient for beach-bar exchange [-]
θ	Wind angle against shore normal [°]
ρ_a	Air density [kg/m^3]
ρ_s	Sand density [kg/m^3]

References

Almström, B., and Fredriksson, C., 2011. *Stranderosion i Ängelholms kommun - Inventering av nuvarande förhållande och rekommendationer för framtiden*. Malmö, Sweden: Sweco (in Swedish), 42 p.

Atkinson, A.L., Baldock, T.E., Birrien, F., Callaghan, D.P., Nielsen, P., Beuzen, T., Turner, I.L., Blenkinsopp, C.E., and Ranasinghe, R., 2018. Laboratory investigation of the Bruun Rule and beach response to sea level rise. *Coastal Engineering* 136, 183–202.

Bagnold, R.A., 1937. The transport of sand by wind. *The Geographical Journal* 89, 409–438.

Bagnold, R.A., 1941. *The physics of blown sand and desert dunes*. London, UK: Meuthen, 263 p.

Bagnold, R.A., 1973. The Nature of Saltation and of "Bed-Load" Transport in Water. *Proceedings of the Royal Society A: Mathematical, Physical and Engineering Sciences* 332, 473–504.

Bailard, J.A., 1982. Modeling on-offshore sediment transport in the surfzone. *Proceedings, International Conference on Coastal Engineering, Cape Town*. ASCE, New York. 1419–1438.

Bakker, M.A.J., van Heteren, S., Vonhögen, L.M., van der Spek, A.J.F., and van der Valk, B., 2012. Recent Coastal Dune Development: Effects of Sand Nourishments. *Journal of Coastal Research* 282, 587–601.

Barchyn, T.E., Martin, R., Kok, J., and Hugenholtz, C.H., 2014. Fundamental mismatches between measurements and models in aeolian sediment transport prediction: The role of small-scale variability. *Aeolian Research* 15, 245–251.

Bascom, W.N., 1951. The relationship between sand size and beach-face slope. *Transactions, American Geophysical Union* 32, 866–874.

Bauer, B.O., and Davidson-Arnott, R.G.D., 2002. A general framework for modeling sediment supply to coastal dunes including wind angle, beach geometry, and fetch effects. *Geomorphology* 49, 89–108.

Bauer, B.O., Davidson-Arnott, R.G.D., Hesp, P., Namikas, S.L., Ollerhead, J., and Walker, I.J., 2009. Aeolian sediment transport on a beach: Surface moisture, wind fetch, and mean transport. *Geomorphology* 105, 106–116.

Belly, P.-Y., 1964. *Sand movement by wind*. Technical Memorandum No. 1, US. Army Corps of Engineers.

Bilskie, M. V, Hagen, S.C., Medeiros, S.C., and Passeri, D.L., 2014. Dynamics of sea level rise and coastal flooding. *Geophysical Research Letters* 41, 927–934.

Booij, N., Ris, R.C., and Holthuijsen, L.H., 1999. A third-generation wave model for coastal regions, Part I, Model description and validation. *Journal of Geophysical Research* 104, 7649–7666.

Borsje, B.W., van Wesenbeeck, B.K., Dekker, F., Paalvast, P., Bouma, T.J., van Katwijk, M.M., and de Vries, M.B., 2011. How ecological engineering can serve in coastal protection. *Ecological Engineering* 37, 113–122.

Bruun, P., 1954. *Coast erosion and the development of beach profiles*. Beach Erosion Board Technical Memorandum. US Army Corps of Engineers, Washington DC 44, 79 p.

Bruun, P., 1962. Sea level rise as a cause of shore erosion. *Journal of the Waterways and Harbors Division Proceedings of the American Society of Civil Engineers* 88, 117–130.

Callaghan, D.P., Nielsen, P., Short, A., and Ranasinghe, R., 2008. Statistical simulation of wave climate and extreme beach erosion. *Coastal Engineering* 55, 375–390.

Christiansen, M.B., and Davidson-Arnott, R., 2004. Rates of Landward Sand Transport over the Foredune at Skallingen, Denmark and the Role of Dune Ramps. *Geografisk Tidsskrift-Danish Journal of Geography* 104, 31–43.

Church, J.A., Clark, P.U., Cazenave, A., Gregory, J.M., Jevrejeva, S., Levermann, A., Merrifield, M.A., Milne, G.A., Nerem, R.S., Nunn, P.D., Payne, A.J., Pfeffer, W.T., Stammer, D., and Unnikrishnan, A.S., 2013. *Sea level change*. Climate Change 2013: The Physical Science Basis. Contribution of Working Group I to the Fifth Assessment Report of the Intergovernmental Panel on Climate Change 1137–1216.

Cooper, J.A.G., and Pilkey, O.H., 2004. Sea-level rise and shoreline retreat: Time to abandon the Bruun Rule. *Global and Planetary Change* 43, 157–171.

Davidson-Arnott, R.G.D., 2005. Conceptual Model of the Effects of Sea Level Rise on Sandy Coasts. *Journal of Coastal Research* 216, 1166–1172.

Davidson-Arnott, R.G.D., and Law, M.N., 1990. *Seasonal patterns and controls on sediment supply to coastal foredunes, Long Point, Lake Erie*. In: Norstrom, K. F., Psuty, P., and Carter, R. W. G. (Eds) Coastal Dunes: Form and Process. Wiley, p. 177–200.

de Vriend, H.J., van Koningsveld, M., Aarninkhof, S.G.J., de Vries, M.B., and Baptist, M.J., 2015. Sustainable hydraulic engineering through building with nature. *Journal of Hydro-Environment Research* 9, 159–171.

de Vries, S., Arens, S.M., de Schipper, M.A., and Ranasinghe, R., 2014a. Aeolian sediment transport on a beach with a varying sediment supply. *Aeolian Research* 15, 235–244.

de Vries, S., Southgate, H.N., Kanning, W., and Ranasinghe, R., 2012. Dune behavior and aeolian transport on decadal timescales. *Coastal Engineering* 67, 41–53.

de Vries, S., van Thiel de Vries, J.S.M., van Rijn, L.C., Arens, S.M., and Ranasinghe, R., 2014b. Aeolian sediment transport in supply limited situations. *Aeolian Research* 12, 75–85.

Dean, R.G., 1977. *Equilibrium beach profiles: U.S. Atlantic and Gulf coasts*, Report No. 12. Department of Civil Engineering, Ocean Engineering. Newark, Delaware: University of Delaware.

Dean, R.G., 1987. Additional sediment input to the nearshore region. *Shore and Beach* 76–81.

Dean, R.G., and Houston, J.R., 2016. Determining shoreline response to sea level rise. *Coastal Engineering* 114, 1–8.

Delgado-Fernandez, I., and Davidson-Arnott, R., 2011. Meso-scale aeolian sediment input to coastal dunes: The nature of aeolian transport events. *Geomorphology* 126, 217–232.

DHI, n.d. Litpack [WWW Document]. URL https://www.mikepoweredbydhi.com/products/litpack (accessed 10.22.18).

Durán, O., Claudin, P., and Andreotti, B., 2011. On aeolian transport: Grain-scale interactions, dynamical mechanisms and scaling laws. *Aeolian Research* 3, 243–270.

Durán, O., and Moore, L.J., 2013. Vegetation controls on the maximum size of coastal dunes. *Proceedings of the National Academy of Sciences of the United States of America* 110, 17217–22.

Fryberger, S.G., and Dean, G., 1979. *Dune Forms and Wind Regimes*. In: McKee, E.D. (Ed.), A Study of Global Sand Seas. Reston, VA, USA: U.S. Geological Survey p. 137–169.

Fryear, D.W., and Saleh, A., 1996. Wind erosion: Field length. *Soil Science* 161, 398–404.

Hallermeier, R.J., 1978. Uses for a calculated limit depth to beach erosion. *Proceeding of the 16th Coastal Engineering Conference,* Hamburg, Germany1493–1512.

Hanson, H., Aarninkhof, S., Capobianco, M., Jimenez, J.A., Larson, M., Nicholls, R.J., and de Vriend, H.J., 2003. Modelling of coastal evolution on yearly to decadal time scales. *Journal of Coastal Research* 790–811.

Hanson, H., Brampton, A., Capobianco, M., Dette, H.H., Hamm, L., Laustrup, C., Lechuga, A., and Spanhoff, R., 2002. Beach nourishment projects, practices, and objectives - A European overview. *Coastal Engineering* 47, 81–111.

Hanson, H., and Kraus, N.C., 1989. *GENESIS: Generalized model for simulating shoreline change.* Report 1 Technical Reference. Vicksburg, Mississippi: U.S. Army Engineer Waterways Experiment Station, Coastal Engineering Research Center. p. 336

Hanson, H., and Larson, M., 2008. Implications of extreme waves and water levels in the southern Baltic Sea. *Journal of Hydraulic Research* 46, 292–302.

Hanson, H., Larson, M., and Kraus, N.C., 2010. Calculation of beach change under interacting cross-shore and longshore processes. *Coastal Engineering* 57, 610–619.

Hardisty, J., and Whitehouse, R.J.S., 1988. Evidence for a new sand transport process from experiments on Saharan dunes. *Letters of Nature* 332, 532–534.

Hesp, P., 1988. Surfzone, beach and foredune interactions on the Australian southest coast. *Journal of Coastal Research* 3, 15–25.

Hesp, P., 2002. Foredunes and blowouts: initiation, geomorphology and dynamics. *Geomorphology* 48, 245–268.

Hoonhout, B.M., and de Vries, S., 2016. A Process-based Model for Aeolian Sediment Transport and Spatiotemporal Varying Sediment Availability. *Journal of Geophysical Research* 121, 1-21

Horikawa, K., 1978. *Coastal Engineering: An Introduction to Ocean Engineering*. Tokyo, Japan: University of Tokyo Press. p.402

Houston, J.R., 2015. Shoreline Response to Sea-Level Rise on the Southwest Coast of Florida. *Journal of Coastal Research* 314, 777–789.

Hsu, S.-A., 1971. Wind stress criteria in eolian sand transport. *Journal of Geophysical Research* 76, 8684–8686.

Inman, D.L., and Bagnold, R.A., 1963. *Littoral processes*. In: Hill, M.N. (Ed.), The Sea. New York: Wiley-Interscience p. 529–553.

Iversen, J.D., and Rasmussen, K.R., 1994. The effect of surface slope on Saltation threshold. *Sedimentology* 41, 721–728.

Kamphuis, J.W., 1991. Alongshore Sediment Transport Rate. *Journal of Waterway, Port, Coastal, and Ocean Engineering* 117, 624–640.

Kawamura, R., 1951. *Study on Sand Movement by Wind*. Reports of Physical Sciences Research Institute of Tokyo University 5(3–4), p. 95–112.

Kraus, N.C., Larson, M., and Wise, R., 1999. Depth of closure in beach-fill design. *Proceedings of the 12th National Conference on Beach Preservation Technology*. American Society of Civil Engineers, 271–286.

Kriebel, D.L., and Dean, R.G., 1993. Convolution method for time-dependent beach-profile response. *Journal of Waterway, Port, Coastal, and Ocean Engineering* 119, 204–226.

Kuriyama, Y., Mochizuki, N., and Nakashima, T., 2005. Influence of vegetation on aeolian sand transport rate from a backshore to a foredune at Hasaki, Japan. *Sedimentology* 52, 1123–1132.

Larson, M., Donnelly, C., Jiménez, J.A., and Hanson, H., 2009. Analytical model of beach erosion and overwash during storms. *Proceedings of the Institution of Civil Engineers - Maritime Engineering* 162, 115–125.

Larson, M., Erikson, L., and Hanson, H., 2004. An analytical model to predict dune erosion due to wave impact. *Coastal Engineering* 51, 675–696.

Larson, M., Hanson, H., and Palalane, J., 2013. Simulating cross-shore material exchange in long-term coastal evolution models. *Proceedings of Coastal Dynamics Conference* 2013.

Larson, M., and Kraus, N.C., 1989. *SBEACH: Numerical model for simulating storm-induced beach change, report 1: empirical foundation and model development*. Technical Report CERC-89-9. Vicksburg, Mississippi: U.S. Army Engineer Waterways Experiment Station, Coastal Engineering Research Center.

Lesser, G.R., Roelvink, J.A., van Kester, J.A.T.M., and Stelling, G.S., 2004. Development and validation of a three-dimensional morphological model. *Coastal Engineering* 51, 883–915.

Lettau, K., and Lettau, H., 1978. E*xperimental and micrometeorological field studies of dune migration*. In: Lettau, H., Lettau, K. (Eds.), Exploring the World's Driest Climate. University of Wisconsin-Madison.

Lincke, D., and Hinkel, J., 2018. Economically robust protection against 21st century sea-level rise. *Global Environmental Change* 51, 67–73.

Lindell, J.;, Fredriksson, C.;, and Hanson, H., 2017. Impact of dune vegetation on wave and wind erosion A case study at Ängelholm Beach, South Sweden. *VATTEN – Journal of Water Management and Research* 73, 39–48.

Line, D.E., Harman, W.A., Jennings, G.D., and Thompson, E.J., 2014. *IPCC: Climate change 2014: synthesis report*. In: Pachauri, R.K., Meyer, L.A. (Eds.), Contribution of

Working Groups I, II and III to the Fifth Assessment Report of the Intergovernmental Panel on Climate Change.

Longuet-Higgins, M.S., and Stewart, R.W., 1964. Radiation stresses in water waves; a physical discussion, with applications. *Deep-Sea Research* 11, 529–562.

Luijendijk, A., De Vroeg, H., Swinkels, C., and Walstra, D.-J.R., 2011. Coastal response on multiple scales: a pilot study on the IJmuiden Port. *Proceedings of the Coastal Sediments Conference* 602–615.

Luijendijk, A., Hagenaars, G., Ranasinghe, R., Baart, F., Donchyts, G., and Aarninkhof, S., 2018. The State of the World's Beaches. *Scientific Reports* 8.

Luna, M.C.M. de M., Parteli, E.J.R., Durán, O., and Herrmann, H.J., 2011. Model for the genesis of coastal dune fields with vegetation. *Geomorphology* 129, 215–224.

McLaren, P., and Bowles, D., 1985. The effects of sediment transport on grain-size distributions. *Journal of Sedimentary Petrology* 55, 457–470.

Miller, J.K., and Dean, R.G., 2004. A simple new shoreline change model. *Coastal Engineering* 51, 531–556.

Neumann, B., Vafeidis, A.T., Zimmermann, J., and Nicholls, R.J., 2015. Future coastal population growth and exposure to sea-level rise and coastal flooding - A global assessment. *PLoS ONE* 10.

Nishi, R., and Kraus, N.C., 1996. Mechanism and calculation of sand dune erosion by storms. *Proceedings of the 25th Coastal Engineering Conference. ASCE*, 3034–3047.

Ollerhead, J., Davidson-Arnott, R., Walker, I.J., and Mathew, S., 2013. Annual to decadal morphodynamics of the foredune system at Greenwich Dunes, Prince Edward Island, Canada. *Earth Surface Processes and Landforms* 38, 284–298.

Overton, M.F., Fisher, J.S., and Young, M.A., 1988. Laboratory investigation of dune erosion. *Journal of Waterway, Port, Coastal and Ocean Engineering* 114, 367–373.

Owen, P., 1964. Saltation of uniform grains in air. *Journal of Fluid Mechanics* 20, 225–242.

Pelnard-Considère, R., 1956. Essai de théorie de l'évolution des formes de rivage en plages de sable et de galets. *4me Journees de l'Hydraulique* 289–298. (in French)

Persson, G., Sjökvist, E., Åström, S., Eklund, D., Andréasson, J., Johnell, A., Asp, M., Olsson, J., and Nerheim, S., 2012. *Klimatanalys för Skåne län.* SMHI Rapport Nr 2011-52, Norrköping, Sweden: SMHI (in Swedish).

Psuty, N.P., 1988. Sediment budget and dune / beach interaction. *Journal of Coastal Research* 3, 1–4.

Ranasinghe, R., Callaghan, D., and Stive, M.J.F., 2012. Estimating coastal recession due to sea level rise: Beyond the Bruun rule. *Climatic Change* 110, 561–574.

Ranwell, D.S., 1972. *Ecology of Salt Marshes and Sand Dunes*. London, UK: Chapman and Hall.

Rijkswaterstaat, 2017. *The yearly coastal measurements* (in Dutch: De JAaRlijkse KUStmetingen or JARKUS).

Robinet, A., Idier, D., Castelle, B., and Marieu, V., 2018. A reduced-complexity shoreline change model combining longshore and cross-shore processes: the LX-Shore model. *Environmental Modelling & Software* 109, 1–16.

Roelvink, D., Reniers, A., van Dongeren, A., van Thiel de Vries, J., McCall, R., and Lescinski, J., 2009. Modelling storm impacts on beaches, dunes and barrier islands. *Coastal Engineering* 56, 1133–1152.

Rosati, J.D., Dean, R.G., and Walton, T.L., 2013. The modified Bruun Rule extended for landward transport. *Marine Geology* 340, 71–81.

Ruessink, B.G., Arens, S.M., Kuipers, M., and Donker, J.J.A., 2018. Coastal dune dynamics in response to excavated foredune notches. *Aeolian Research* 31, 3–17.

Sallenger, A.H., 2000. Storm impact scale for barrier islands. *Journal of Coastal Research* 16, 890–895.

Sauermann, G., Kroy, K., and Herrmann, H.J., 2001. Continuum saltation model for sand dunes. *Physical review. E, Statistical, nonlinear, and soft matter physics* 64, 031305.

Self, R.P., 1977. Longshore Variation in Beach Sands Nautla Area, Veracruz, Mexico. *Journal of Sedimentary Research* 47, 1437–1443.

Seymour, R.J., and Castel, D., 1989. *Modeling cross-shore transport*. In: Seymour, R.J. (Ed.), Nearshore Sediment Transport. New York: Plenum Press, p. 387–401.

Shepard, F.P., 1950. *Beach cycles in S. California,* Technical Memo, 20, 26, US Army Corps of Engineers.

Sherman, D.J., and Bauer, O., 1993. Dynamics of beach-dune systems. *Progress in Physical Geography* 17, 413–447.

Sherman, D.J., Jackson, D.W.T., Namikas, S.L., and Wang, J., 1998. Wind-blown sand on beaches: an evaluation of models. *Geomorphology* 22, 113–133.

Sherman, D.J., Li, B., Ellis, J.T., Farrell, E.J., Maia, L.P., and Granja, H., 2013. Recalibrating aeolian sand transport models. *Earth Surface Processes and Landforms* 38, 169–178.

Short, A.D., and Hesp, P.A., 1982. Wave, beach and dune interactions in southeastern Australia. *Marine Geology* 48, 259–284.

Steetzel, H.J., 1993. *Cross-shore Transport during Storm Surges*. Ph. D. Thesis. Delft, the Netherlands: Delft University of Technology

Stive, M.J.F., Aarninkhof, S.G.J., Hamm, L., Hanson, H., Larson, M., Wijnberg, K.M., Nicholls, R.J., and Capobianco, M., 2002. Variability of shore and shoreline evolution. *Coastal Engineering* 47, 211–235.

Stout, J.E., 1990. Wind erosion within a simple field. *Transactions of the American Society of Agricultural Engineers* 33, 1597– 1600.

Tonnon, P.K., Huisman, B.J.A., Stam, G.N., and Van Rijn, L.C., 2018. Numerical modelling of erosion rates, life span and maintenance volumes of mega nourishments. *Coastal Engineering* 131, 51–69.

Trask, C.B., and Hand, B.M., 1985. Differential transport of fall-equivalent sand grains, Lake Ontario, New York. *Journal of Sedimentary Petrology* 55, 226–234.

USACE, (US Army Corps of Engineers), 1984. *Shore Protection Manual* (SPM). Washington: U.S. Government Printing Office.

van Boxel, J.H., Arens, S.M., and van Dijk, P.M., 1999. Aeolian processes across transverse dunes. I: Modelling the air flow. *Earth Surface Processes and Landforms* 24, 255–270.

van der Wal, D., 2004. Beach-Dune Interactions in Nourishment Areas along the Dutch Coast. *Journal of Coastal Research* 201, 317–325.

van Dijk, P.M., Arens, S.M., and van Boxel, J.H., 1999. Aeolian processes across transverse dunes. II: Modelling the sediment transport and profile development. *Earth Surface Processes and Landforms* 24, 319–333.

van Duin, M.J.P., Wiersma, N.R., Walstra, D.J.R., van Rijn, L.C., and Stive, M.J.F., 2004. Nourishing the shoreface: Observations and hindcasting of the Egmond case, The Netherlands. *Coastal Engineering* 51, 813–837.

van Rijn, L.C., 1997. Sediment transport and budget of the central coastal zone of Holland. *Coastal Engineering* 32, 61–90.

Vellinga, P., 1986. *Beach and dune erosion during storm surges*. Publication 372, Delft Hydraulics Ph. D. Thesis, Delft, the Netherlands: Delft University of Technology

Vitousek, S., Barnard, P.L., Limber, P., Erikson, L., and Cole, B., 2017. A model integrating longshore and cross-shore processes for predicting long-term shoreline response to climate change. *Journal of Geophysical Research: Earth Surface* 122, 782–806.

Wainwright, D.J., Ranasinghe, R., Callaghan, D.P., Woodroffe, C.D., Jongejan, R., Dougherty, A.J., Rogers, K., and Cowell, P.J., 2015. Moving from deterministic towards probabilistic coastal hazard and risk assessment: Development of a modelling framework and application to Narrabeen Beach, New South Wales, Australia. *Coastal Engineering* 96, 92–99.

Weng, W.S., Hunt, J.C.R., Carruthers, D.J., Warren, A., Wiggs, G.F.S., Livingstone, I., and Castro, I., 1991. Air flow and sand transport over sand-dunes. *Acta Mechanica* 2, 1–22.

Wijnberg, K.M., 2002. Environmental controls on decadal morphologic behaviour of the Holland coast. *Marine Geology* 189, 227–247.

Wong, P.P., Losada, I.J., Gattuso, J.P., Hinkel, J., Khattabi, A., McInnes, K.L., Saito, Y., Sallenger, A., Nicholls, R.J., Santos, F., and Amez, S., 2015. *Coastal systems and low-lying areas*. In: Climate Change 2014 Impacts, Adaptation and Vulnerability: Part A: Global and Sectoral Aspects.

Wright, L.D., and Short, A.D., 1984. Morphodynamic variability of surf zones and beaches: A synthesis. *Marine Geology* 56, 93–118.

Yates, M.L., Guza, R.T., O'Reilly, W.C., Hansen, J.E., and Barnard, P.L., 2011. Equilibrium shoreline response of a high wave energy beach. *Journal of Geophysical Research: Oceans* 116, 1–13.

Zhang, W., Schneider, R., Kolb, J., Teichmann, T., Dudzinska-Nowak, J., Harff, J., and Hanebuth, T.J.J., 2015. Land-sea interaction and morphogenesis of coastal foredunes - A modeling case study from the southern Baltic Sea coast. *Coastal Engineering* 99, 148-166.

Zingg, A., 1953. Wind tunnel studies of the movement of sedimentary material. *Proceedings of the 5th Hydraulic Conference Bulletin* 34, 111–135.

Caroline Hallin is a coastal engineer with a master's degree in environmental engineering. Before pursuing a PhD at Lund University, she was working as a consultant engineer in river and coastal engineering. Her primary expertise is within sediment transport and coastal evolution, flood risk analysis, and coastal protection and planning. Caroline is engaged in several coastal networks in Sweden and abroad; she founded a coastal section in the Swedish Association for Water where she is also involved in the board. During her PhD, Caroline has organised three coastal conferences in Sweden and given many talks at scientific meetings and public venues. She is engaged in raising awareness about the local problems with coastal flooding and erosion in south Sweden and has written debate articles and appeared in newspapers, radio, and television to educate the public about coastal processes, risks and mitigation methods.

Faculty of Engineering
Lund University
ISBN 978-91-7895-062-1

LUND
UNIVERSITY